AWARD NUMBER: W81XWH-20-1-0683

TITLE: Identifying Novel Therapeutic Targets and Combination Strategies for Patients with BPDCN

PRINCIPAL INVESTIGATOR: Naveen Pemmaraju

CONTRACTING ORGANIZATION: The University of Texas MD Anderson Cancer Center
Houston, TX

REPORT DATE: October 2022

TYPE OF REPORT: Annual

PREPARED FOR: U.S. Army Medical Research and Development Command
Fort Detrick, Maryland 21702-5012

DISTRIBUTION STATEMENT: Approved for Public Release; Distribution Unlimited

REPORT DOCUMENTATION PAGE

Form Approved
OMB No. 0704-0188

1. REPORT DATE	2. REPORT TYPE	3. DATES COVERED
October 2022	Annual	30Sep2021-29Sep2022

4. TITLE AND SUBTITLE

Identifying Novel Therapeutic Targets and Combination Strategies for Patients with BPDCN

5a. CONTRACT NUMBER

5b. GRANT NUMBER
W81XWH-20-1-0683

5c. PROGRAM ELEMENT NUMBER

6. AUTHOR(S)
Marina Konopleva, MD, PhD, Andrew Lane, MD, Omar Abdel-Wahab, MD, Naveen Pemmaraju

E-Mail: mkonople@mdanderson.org, Andrew_Lane@DFCI.HARVARD.EDU, abdelwao@mskcc.org

5d. PROJECT NUMBER

5e. TASK NUMBER

5f. WORK UNIT NUMBER

7. PERFORMING ORGANIZATION NAME(S) AND ADDRESS(ES)
The University of Texas MD Anderson Cancer Center, 1515 Holcombe Blvd., Houston, TX 77030
Dana-Farber Cancer Institute, 450 Brookline Avenue, Boston, MA 02215
Memorial Sloan Kettering Cancer Center, 1275 York Avenue, New York, NY 10065

8. PERFORMING ORGANIZATION REPORT NUMBER

9. SPONSORING / MONITORING AGENCY NAME(S) AND ADDRESS(ES)

U.S. Army Medical Research and Development Command
Fort Detrick, Maryland 21702-5012

10. SPONSOR/MONITOR'S ACRONYM(S)

11. SPONSOR/MONITOR'S REPORT NUMBER(S)

12. DISTRIBUTION / AVAILABILITY STATEMENT

Approved for Public Release; Distribution Unlimited

13. SUPPLEMENTARY NOTES

14. ABSTRACT Project 1: We used CRISPR interference to perform an unbiased assessment of genes that confer sensitivity or resistance to tagraxofusp or to venetoclax and azacitidine when knocked down. We compared these data to RNA-sequencing of BPDCN cells at baseline and in the setting of MRD after treatment with the same drug. We identified hits in expected pathways that mediate resistance to venetoclax and tagraxofusp. One important hit was a largely uncharacterized RNA binding protein that confers sensitivity to both treatments when depleted. We performed eCLIP-seq to identify targets of this RNA binding protein and are currently performing experiments to understand the mechanism of sensitization. Project 2. We expanded efficacy study of the combination of IMGN632/VEN/AZA. By using large scale drug screen followed by BLISS independence analysis, we confirmed that triple treatment is synergistic at multiple of dosage levels and ratios in AML cell lines and primary samples. Mechanistically, BH3 profiling indicated that IMGN632 alone significantly primed AML cells to venetoclax-induced apoptosis, providing a strong rationale for tested combination. We also showed that IMGN632-indued DNA damage resulted in cell cycle arrest, blockade of DNA synthesis and activation of DNA damage response (DDR). Importantly, venetoclax impaired DDR triggered by IMGN632, which may additionally account for the increased efficacy of IMGN632/VEN combination. At clinical level, we opened the expansion cohorts for patients with BPDCN using the RPD2 of TAG/AZA/VEN: one cohort for first line treatment and second one for relapsed or refractory BPDCN. To date, 6 patients with r/r BPDCN and one patient with previously untreated BPDCN has been enrolled. Complete responses (CRs) were observed in 4 of 6 patients with r/r BPDCN who further proceeded to stem cell transplantation. All four patients had received prior single agent TAG, which is very encouraging for our mechanistic hypothesis for overcoming TAG resistance. To date we have enrolled 2 patients with previously untreated BPDCN. Project Aim 3: Aim identified the impact of mutations in the RNA splicing factor ZRSR2 in BPDCN including global impact of these mutations on RNA splicing and RNA binding. We also performed functional genomic screens to identify the basis for enrichment of *ZRSR2* mutations in BPDCN. Moreover, we identified new therapeutic

means to modulate RNA splicing for therapeutic benefit in BPDCN. Importantly, some of these modalities were found to synergize with BCL2 inhibition and promote the efficacy of venetoclax.

15. SUBJECT TERMS

Blastic Plasmacytoid Dendritic Cell Neoplasm (PBDCN), Acute Myeloid Leukemia (AML), CD123, tagraxofusp, IMGN632, venetoclax, azacytidine, combination therapy,

16. SECURITY CLASSIFICATION OF:			**17. LIMITATION OF ABSTRACT**	**18. NUMBER OF PAGES**	**19a. NAME OF RESPONSIBLE PERSON** USAMRDC
a. REPORT	**b. ABSTRACT**	**c. THIS PAGE**			**19b. TELEPHONE NUMBER** *(include area code)*
Unclassified	Unclassified	Unclassified	Unclassified	41	

Standard Form 298 (Rev. 8-98)
Prescribed by ANSI Std. Z39.18

TABLE OF CONTENTS

1. INTRODUCTION:

BPDCN is a highly aggressive hematologic malignancy characterized by poor clinical outcomes and no approved or standard therapies. It can evolve out of an underlying myelodysplastic syndrome or present de novo. The median age is ~65 years with overall survival of 8-14 months using conventional chemotherapy. Thus, there is an urgent unmet need for rational targeted agents and non-cytotoxic therapies. CD123 (the IL3 receptor) is highly expressed in ~100% of BPDCN cases, generally at higher levels than normal cells or forms of acute myeloid leukemia (AML). This observation led to a multi-center Phase I/II trial of SL-401 (Tagraxofusp) in BPDCN, which our sites led and recent FDA approval of tagraxofusp (Elzonris^{TM}, Stemline Therapeutics, Inc.), a CD123-directed cytotoxin. Among 45 patients, we observed a 72% combined rate of complete response (CR)/clinical complete response in frontline-treated patients and 38% in relapsed patients; 45% of frontline patients were bridged to stem cell transplant.[4] However, many patients experience relapse after initial response to tagraxofusp, and ~30% of patients do not respond to tagraxofusp monotherapy up-front. Preliminary studies indicate that BPDCN is dependent on BCL-2. In BPDCN cell lines, patient samples, patient-derived xenograft (PDX) models, and a two-patient pilot study, we observed a high sensitivity to the BCL-2 inhibitor venetoclax. Since then, there have been subsequent reports of clinical activity against BPDCN with venetoclax as a single agent, or in combination with hypomethylating agents. Although we have observed activity of anti-CD123 and anti-BCL-2 targeted agents as *monotherapies*, relapses still occur in most cases. **This project aims to** investigate mechanisms of response and resistance to the most advanced targeted therapies in BPDCN, assess potential for combination treatment in a clinical trial, and explore novel mechanism-based therapies targeting recurrently mutated genes in BPDCN involved in RNA splicing. **We expect our aims to provide clinical data for the next front-line treatment strategy for BPDCN patients and the preclinical basis to intelligently select the next targeted therapy approach for clinical testing in BPDCN**.

2. KEYWORDS:

Blastic Plasmacytoid Dendritic Cell Neoplasm (PBDCN), Acute Myeloid Leukemia (AML), CD123, tagraxofusp, IMGN632, venetoclax, azacytidine, combination therapy

3. ACCOMPLISHMENTS:

What were the major goals of the project?

Specific Aim 1

Major Task 1: Test the hypothesis that in vivo resistance to tagraxofusp in BPDCN cells is mediated by epigenetic silencing of diphthamide synthesis genes.

Major Task 2: Test the hypothesis that azacitidine cooperates with tagraxofusp in primary BPDCN cells in vivo via its effects on DNA methylation and expression of diphthamide synthesis genes.

Specific Aim 2
Major Task 1 Test the hypothesis that targeting of CD123 with tagraxofusp or IMGN-623 primes BPDCN cells for apoptosis when combined with BCL2 inhibitor venetoclax and AZA.
Major Task 2 Determine the efficacy of combining anti-CD123 therapy with AZA/venetoclax in vivo
Major Task 3 Conduct a Phase 1b/2 clinical trial combining azacitidine, tagraxofusp, and venetoclax in patients with relapsed/refractory BPDCN and frontline patients unfit for induction chemotherapy

Specific Aim 3
Major Task 1: Determine the effects of perturbing splicing in BPDCN models with or without mutations in *ZRSR2* or *SRSF2*.
Major Task 2: Determine aberrant splicing events generated by mutant *ZRSR2* and *SRSF2* in BPDCN which promote transformation through a positive enrichment CRISPR screen.

What was accomplished under these goals?

Specific Aim 1, Major Tasks 1 and 2:

In this reporting period, evaluated and validated the results of our CRISPR interference screen to perform an unbiased assessment of genes that determine sensitivity and resistance to tagraxofusp, azacitidine, and venetoclax in BPDCN. We had two arms in this genome-wide screen using the Dolcetto CRISPRi library completed in collaboration with the Broad Institute Genome Perturbation Platform. We treated library-expressing CAL1 BPDCN cells with TAG or with AZA/VEN and collected cells at a timepoint (72 hours) and dose where there was 8-10-fold enrichment of untreated to treated cells.

QC of the barcoded DNA library enrichment by PCR met all quality parameters and guides were sequenced. Initial data are below, in which we looked for expected genes and lack of hits among the negative controls. First, we analyzed genes associated with VEN/AZA sensitivity and resistance when knocked down (**Figure 1**). We found several expected genes, which validated our screen. These include increased VEN/AZA sensitivity upon knockdown of the antiapoptotic genes MCL1 or BCL2L1, and the TP53 regulator MDM2. Conversely, we found expected resistance to VEN/AZA with knockdown of the pro-apoptotic gene BAX or the cell death regulator TP53.

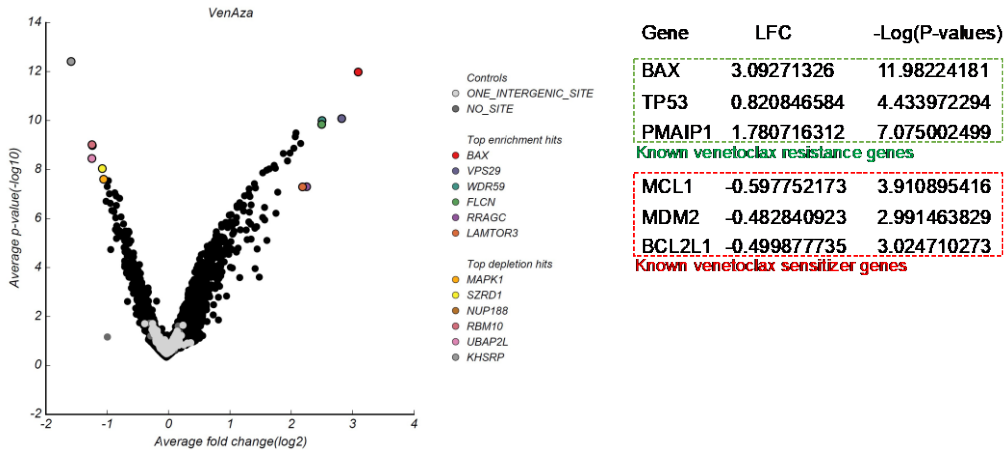

Gene	LFC	-Log(P-values)
BAX	3.09271326	11.98224181
TP53	0.820846584	4.433972294
PMAIP1	1.780716312	7.075002499

Known venetoclax resistance genes

MCL1	-0.597752173	3.910895416
MDM2	-0.482840923	2.991463829
BCL2L1	-0.499877735	3.024710273

Known venetoclax sensitizer genes

Figure 1. Volcano plot of CRISPRi sgRNAs after VEN/AZA treatment showing enrichment (positive fold change, confers resistance when knocked down) and depletion (negative fold change, confers sensitivity when knocked down). Negative controls are in gray (no known site). Several of the significant hits are expected based on known venetoclax sensitivity/resistance genes, as shown on right.

Next, we analyzed resistance and sensitization to TAG in the same way (**Figure 2**). TAG delivers diphtheria toxin to cells via the IL3 receptor. We found that, as expected, resistance to TAG was conferred by knockdown of the IL3-receptor components IL3RA (alpha chain) or CSF2RB (beta chain). Also, as we previously published (Togami et al, JCI 2019), knockdown of the diphthamide components DPH1 or DNAJC24 (aka DPH4) also conferred resistance. This validated the drug screen with TAG treatment with these expected "positive controls."

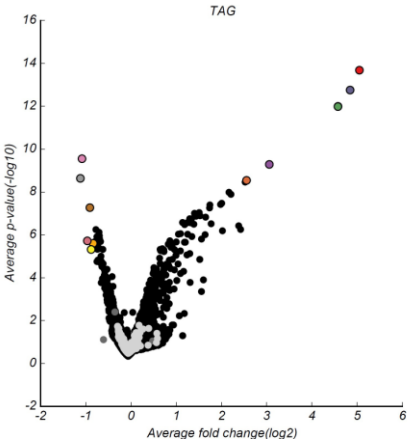

Gene	LFC	-Log(P-values)	
CSF2RB	5.050081485	13.68216092	IL3 receptors
IL3RA	4.84466939	12.75639495	
DNAJC24	4.57672316	11.9954586	Diphthamide pathway
DPH1	4.575489597	11.98523226	

Figure 2. Volcano plot of CRISPRi sgRNAs after TAG treatment showing enrichment (positive fold change, confers resistance when knocked down) and depletion (negative fold change, confers sensitivity when knocked down). Negative controls are in gray (no known site). Several of the significant hits are expected based on known TAG resistance genes, as shown on right.

Next, we focused on sensitization and resistance hits that were shared between TAG and VEN/AZA, because we are now testing the triplet TAG/VEN/AZA in patients (Aim 2) and therefore we want to

understand shared mechanisms of sensitivity and resistance that may be unique to BPDCN. We found that there were 66 genes that were common hits for conferring TAG and VEN/AZA resistance. We performed gene set enrichment analysis on these common genes and found significant hits in control of translation including elongation and termination (**Figure 3**). And on the opposite side, there was one gene that was the most depleted gene in both treatment arms (implying that its knockdown confers sensitivity to both treatments. That was KHSRP, which is a relatively understudied RNA binding protein that is known to control mRNA translation including elongation and termination. Also of interest, we cross-referenced KHSRP against other datasets including our own and found that it is not enriched or depleted in BPDCN genetic perturbation screens in the absence of drug. This suggests that KHSRP is not simply a global dependency that would be depleted in any screen, and instead is specific to the setting of drug treatment. Also, we compared to a published AML CRISPR screen for cytarabine resistance, and it was not a hit, despite the resistant AML cells having some shared signatures such as a high oxidative phosphorylation (OX PHOS) gene enrichent, just as our resistant BPDCN cells do (not shown). Therefore, we are excited about studying the biology of KHSRP in mediating treatment resistance in BPDCN.

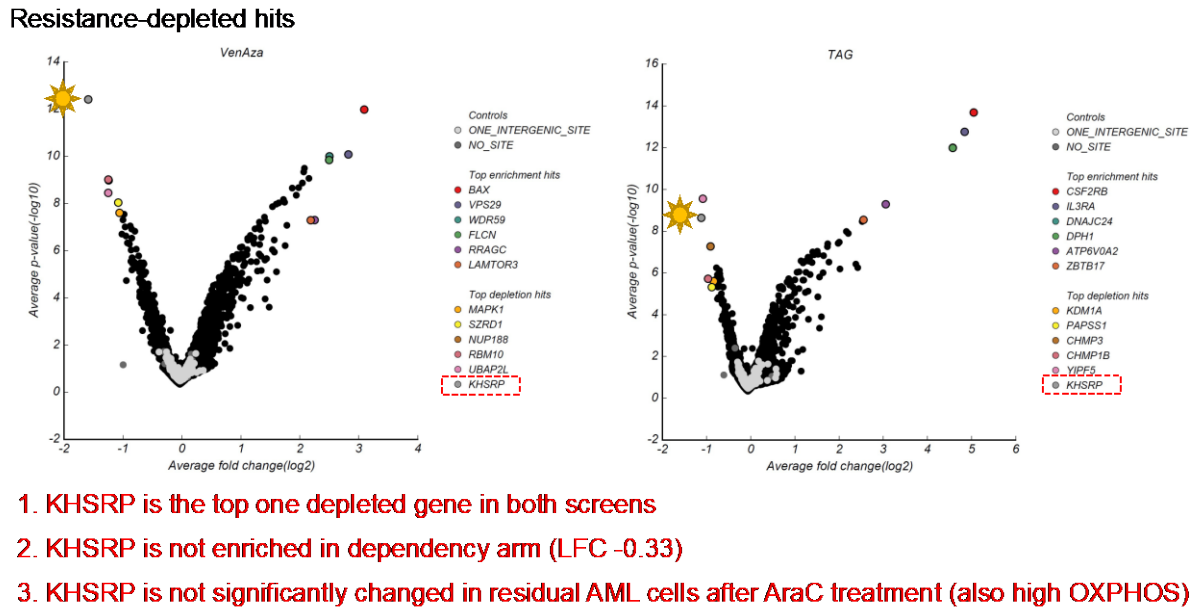

1. KHSRP is the top one depleted gene in both screens
2. KHSRP is not enriched in dependency arm (LFC -0.33)
3. KHSRP is not significantly changed in residual AML cells after AraC treatment (also high OXPHOS) [1,2]

Figure 3. (Top) enriched gene ontology terms among genes that conferred resistance to both TAG and VEN/AZA. (Bottom) KHSRP is the top depleted hit (loss confers sensitivity) to both TAG and VEN/AZA in BPDCN cells, but it is not a dependency in cells without drug treatment nor was it enriched in a prior AML cyatarbine (AraC) sensitivity screen.

We also performed formal synergy testing between venetoclax and azacitidine in two BPDCN cell lines: CAL1 and DF-DCN-86. Most studies using these drugs in BPDCN have only tested the agents singly. We found that there is true synergy, not simply additivity, between the two drugs (**Figure 4**). The effect was seen in both cell lines. Since VEN/AZA is used always as a combination in patients with leukemia, and in our BPDCN clinical trial (Aim 2), this was important to establish the relative concentrations of each that maximized synergy. We used these maximal synergistic doses for designing the next in vitro and in vivo PDX treatment experiments. We also added TAGraxofusp to

the same assays to test if there was additional synergy. Interestingly, we found that TAG and AZA or TAG and VEN are synergistic, TAG plus VEN/AZA was only slightly synergistic and may be more of an additive effect. These are important considerations as we design doublet and triplet treatment approaches for BPDCN.

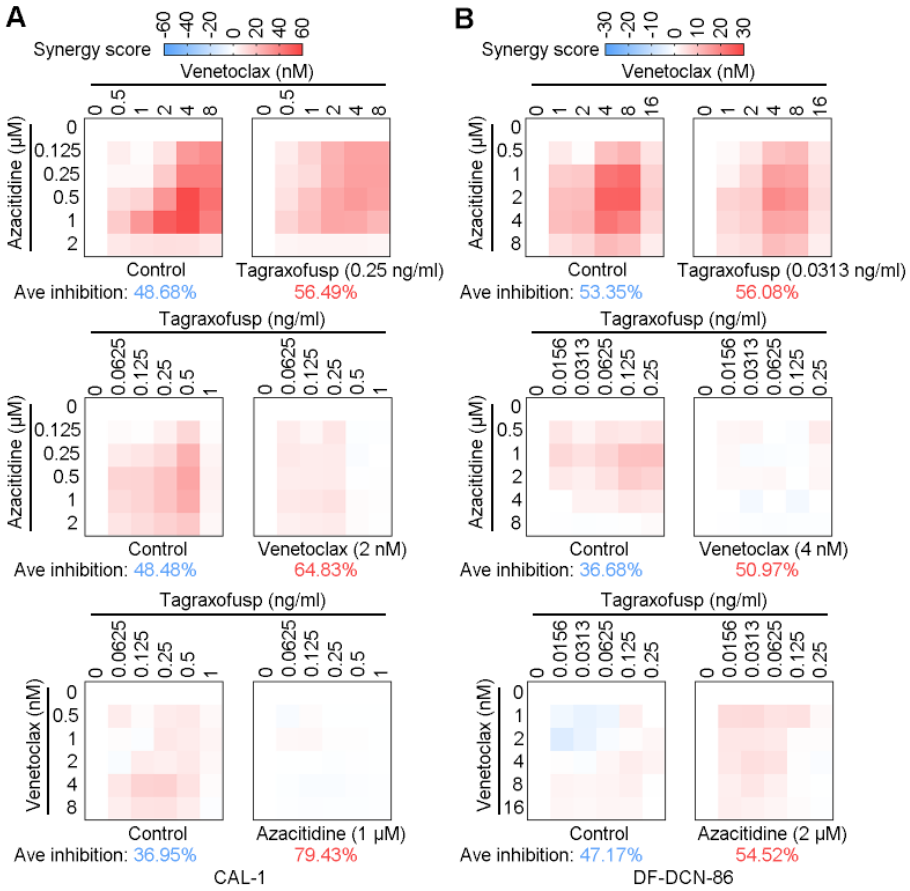

Figure 4. Combination drug treatment experiments in two BPDCN cell lines, CAL1 and DF-DCN-86. Various doublet and triplet combinations of TAG, AZA, and VEN are as shown. Positive scores are in red (>0) and indicate synergy. Negative scores (in blue) indicate antagonism. Additive effects would read near zero in this assay.

Next, we performed a BPDCN PDX treatment experiment with 3 independent patient-derived xenografts, treated with vehicle, VEN+AZA, or TAG. The schema for the VEN+AZA arms are shown below in **Figure 5**. We harvested bone marrow after treatment with vehicle ('primary'), 2 days after VEN/AZA at the low point of residual disease, and 6 weeks later at the time of frank relapse. We purified human CD45+ cells and performed RNA seq.

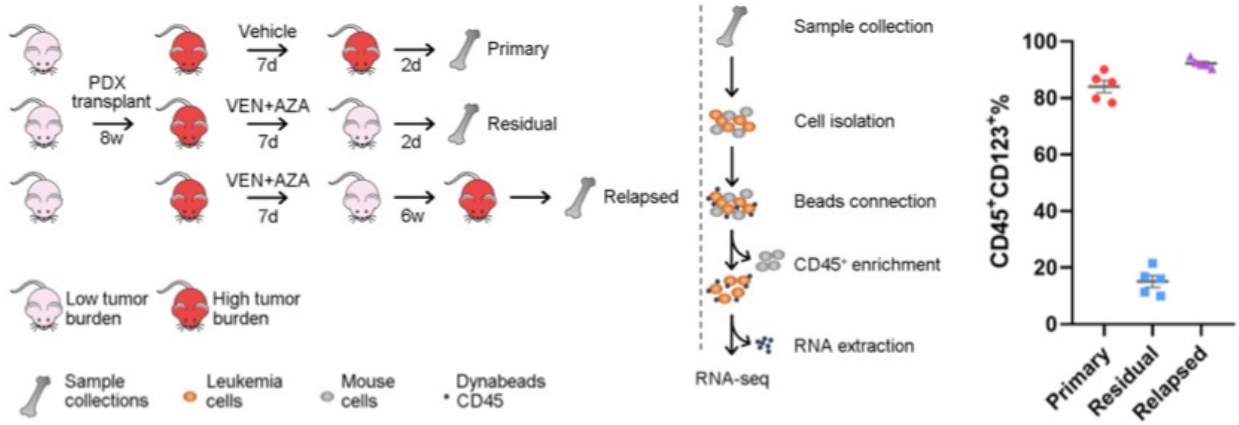

Figure 5. Schema of the in vivo BPDCN PDX treatment experiment to collect early residual disease and relapsed leukemia after VEN/AZA.

We have performed initial analysis of the RNA-seq data (**Figure 6**). Quality was technically very good. Principal component analysis shows that there were distinct clusters of primary, residual, and relapsed disease. Of interest, the majority of the variance between the groups was in the residual disease cells compared to either the primary or the relapsed samples, with fewer differences between primary and relapsed disease. This justifies the importance of examining the residual disease for novel biology. GSEA comparing each subgroup has identified changes in cell cycle (G2M checkpoint and E2F targets) between subgroups, as well as biological signatures such as upregulation of oxidative phosphorylation in residual cells compared to either primary or relapsed cells. Some of these data are consistent with what has been reported for single agent VEN or AZA resistance and some is distinct.

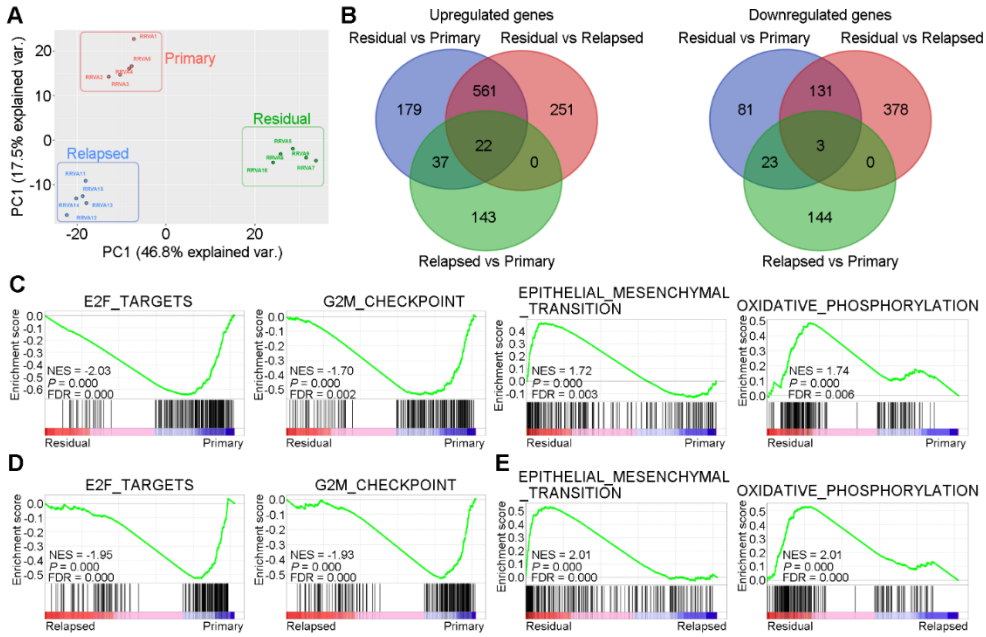

Figure 6. Analysis of RNAseq data from BPDCN PDXs before (primary), 2 days after at the point of minimal bone marrow disease (residual), and 6 weeks later at the time of frank relapse (relapsed). A. Principal component analysis. B. Venn diagrams of the significant up and downregulated genes in each subgroup. C-E. Gene set enrichment analysis of the indicated populations showing cell cycle and metabolic signatures.

We further validated the hits from our drug sensitivity/resistance screen focusing on KHSRP. KHSRP is an RNA binding protein that when knocked down was enriched among BPDCN cells that persisted after VEN/AZA or SL-401. We performed validation experiments with 5 independent sgRNAs for CRISPRi confirming that knockdown conferred sensitivity to both treatments. Importantly, knockdown of KHSRP in the absence of drug treatment did not cause any growth disadvantage. This suggests that KHSRP is not simply a global dependency in BPDCN cells. This is also consistent with our CRISPRi screen data in which KHSRP guides were not depleted in cells propagated in normal growth media (**Figure 7**).

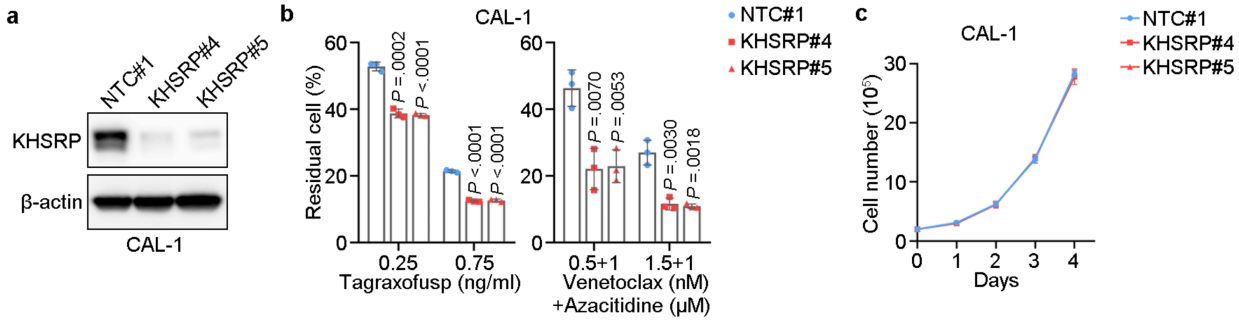

Figure 7. a) CRISPRi knockdown for KHSRP with two independent sgRNAs in CAL-1 BPDCN cells. b) KHSRP knockdown sensitizes to TAG (SL401) and VEN/AZA. C) KHSRP knockdown does not affect CAL-1 growth in normal conditions.

We also performed formal synergy testing between azacitidine and venetoclax in BPDCN cells with and without KHSRP knockdown. AZA and VEN are synergistically toxic to BPDCN cells. But the degree of synergy increases in CAL-1 BPDCN cells treated with the combination of venetoclax and azacitidine. (**Figure 8**).

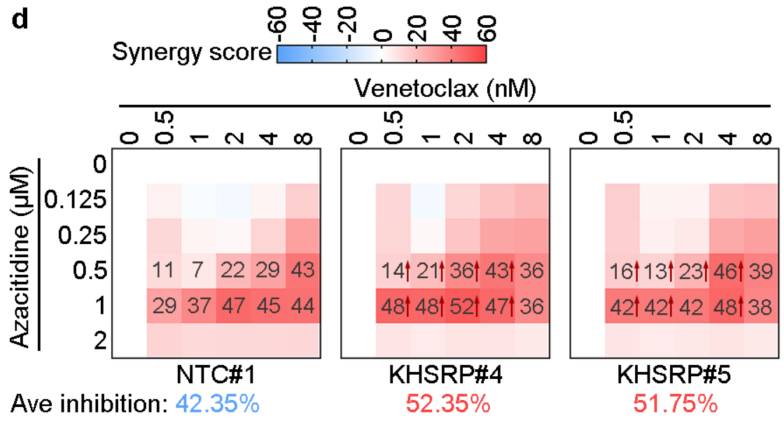

Figure 8. Bliss synergy scores of azacitidine and venetoclax with control sgRNAs or two independent KHSRP1 sgRNAs. Higher numbers and more red color signifies increased synergy.

Finally, we optimized a bench protocol and tested three independent KHSRP antibodies to perform eCLIP-seq (enhanced Cross-Linking and ImmunoPrecipitation) in BPDCN cells. Optimization included determining cell type specific best strategies for cell fixation, UV crosslinking, lysis, immunoprecipitation, reversal of crosslinking, etc. We were successful in obtaining specific pull down of biotinylated RNA fragments that are putative interactors with KHSRP in cells (**Figure 3**). We then performed eCLIP-seq in BPDCN cells at baseline or treated with VEN/AZA, in biological duplicates. From these, we generated RNA sequencing libraries, which are now undergoing 50 basepair single-end Illumina sequencing to 50 million reads/sample.

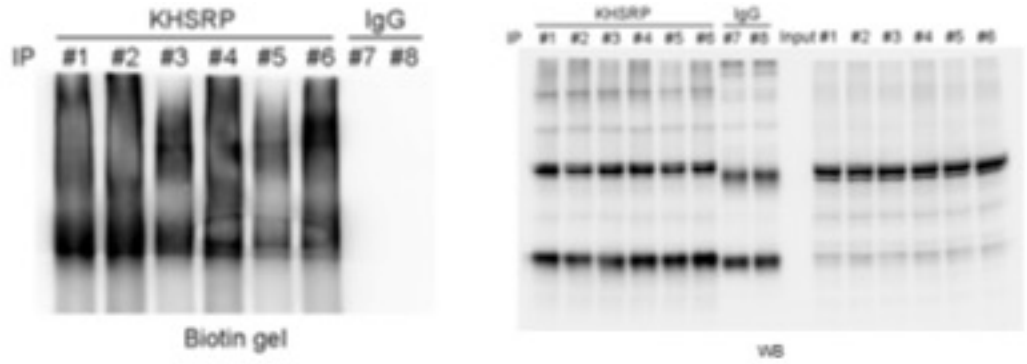

Figure 9. Left – Streptavidin-HRP detection of biotinylated RNAs pulled down by KHSRP antibodies but not by control IgG. Right – western blotting for KHSRP in IP samples and in input cell lysates.

We have begun to analyze eCLIP-seq data in collaboration with bioinformatics colleagues. There are relatively few mRNAs that meet statistical threshold for binding to KHSRP (~100-200 depending on threshold), which was somewhat surprising but is a good sign that we may be able to functionally interrogate many of them for effects on BPDCN drug sensitivity by modulating their level. Analysis is ongoing and will continue in the next funding period.

Specific Aim 2, Major Task 1: Test the hypothesis that targeting of CD123 with tagraxofusp or IMGN-623 primes BPDCN cells for apoptosis when combined with BCL2 inhibitor venetoclax and AZA.

We have previously shown that IMGN632/VEN/AZA combination is synergistic in AML and BPDCN cell lines by testing pharmacological interactions using Chau-Talalay Combination Index (CI) method. In current reporting period, we expanded these studies by designing large scale drug combination screen using BLISS independence model. This allowed us to examine multiple doses of combination of IMGN, VEN and AZA. MV4-11, MOLM13 and MOLM14 AML cells were treated each compound, either individually or in all possible permutations in a checkerboard fashion. Cell growth was asseded by CellTiter-Glo assay. Synergistic interactions were assessed using Combenefit software. BLISS index values for each dose combination >0 represented synergy, whereas BLISS index values <0 represent edantagonism. As shown on the heat maps (Figure 1), while IMGN632+AZA, IMGN+VEN or VEN+AZA were only slightly synergistic, triple combination of IMGN/VEN/AZA was synergistic at multiple dosage levels and ratios with the profound effect observed at higher doses of IMGN632 (10 ng/mL).

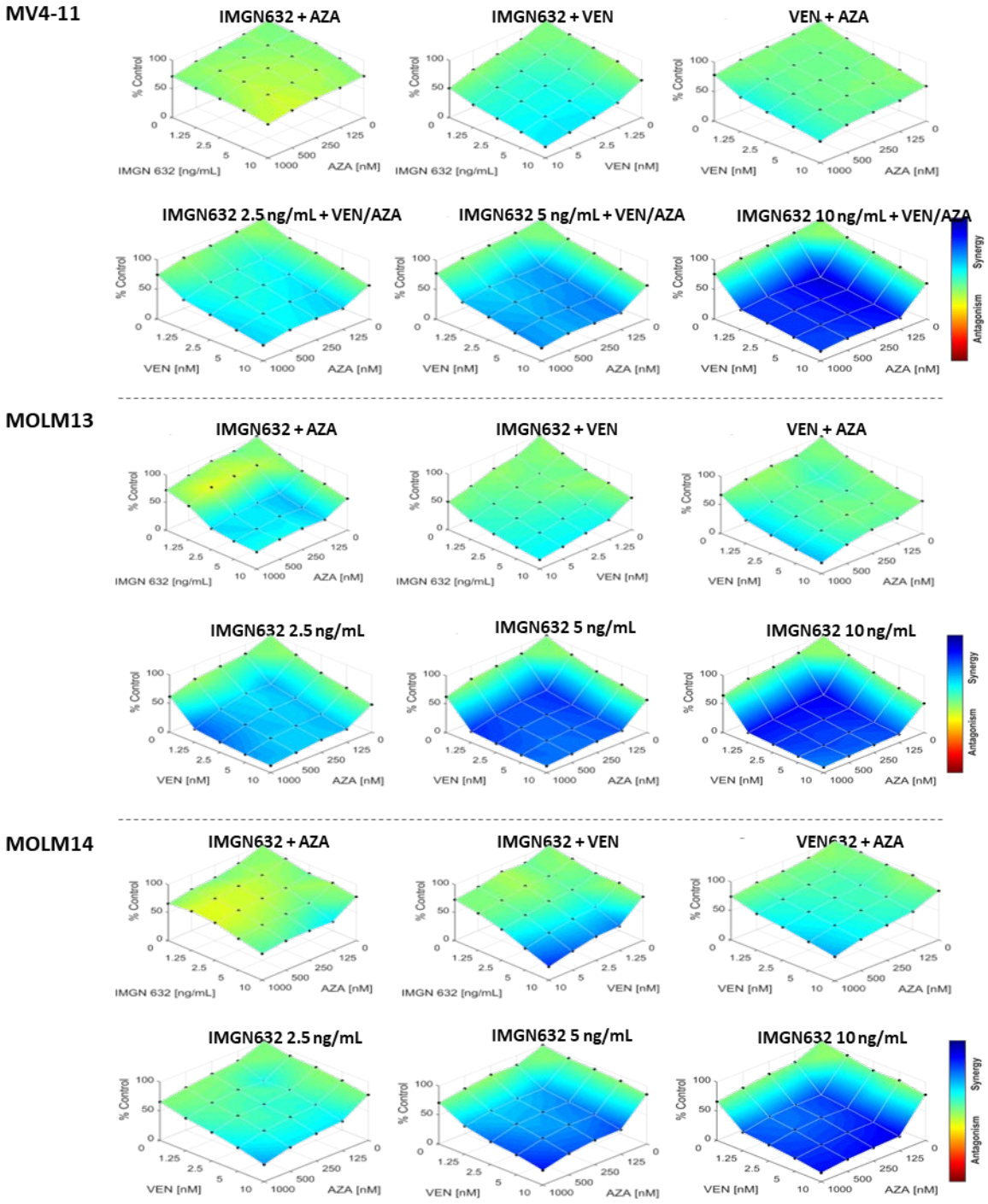

Figure 1. Representative synergistic interactions between IMGN632 combined with VEN and AZA in human AML cells. Cells were treated with IMGN632 for 24h and subsequently exposed for additional 24h to 2-fold serial dilutions of VEN and AZA, either individually or in all possible

permutations in a checkerboard fashion. Cell growth was asseded by CellTiter-Glo assay. Synergistic interactions were assessed using BLISS Independence model. BLISS index values for each dose combination >0 represent synergy, whereas BLISS index values <0 represent antagonism.

Next, we expanded *in vitro* studies by testing IMGN632/VEN/AZA combination in primary AML patients' samples (Figure 2). AML cells were pre-treated with IMGN632 for 48 h and VEN+AZA was added for additional 24 h. Cell viability was measured using CTG assay. Samples, before treatment were screened for CD-123 expression using anti-CD-123-PE and subjected to flow cytometry analysis. Although we are still optimizing the best treatment conditions and doses, it is already visible that AML cells with high level of CD-123 were most sensitive to IMGN632 alone as well as to combined IMGN632/VEN/AZA treatment (samples #1, 2, 3). Cells with low expression of CD-123 (below 2000 molecules/cell), did not respond to combination.

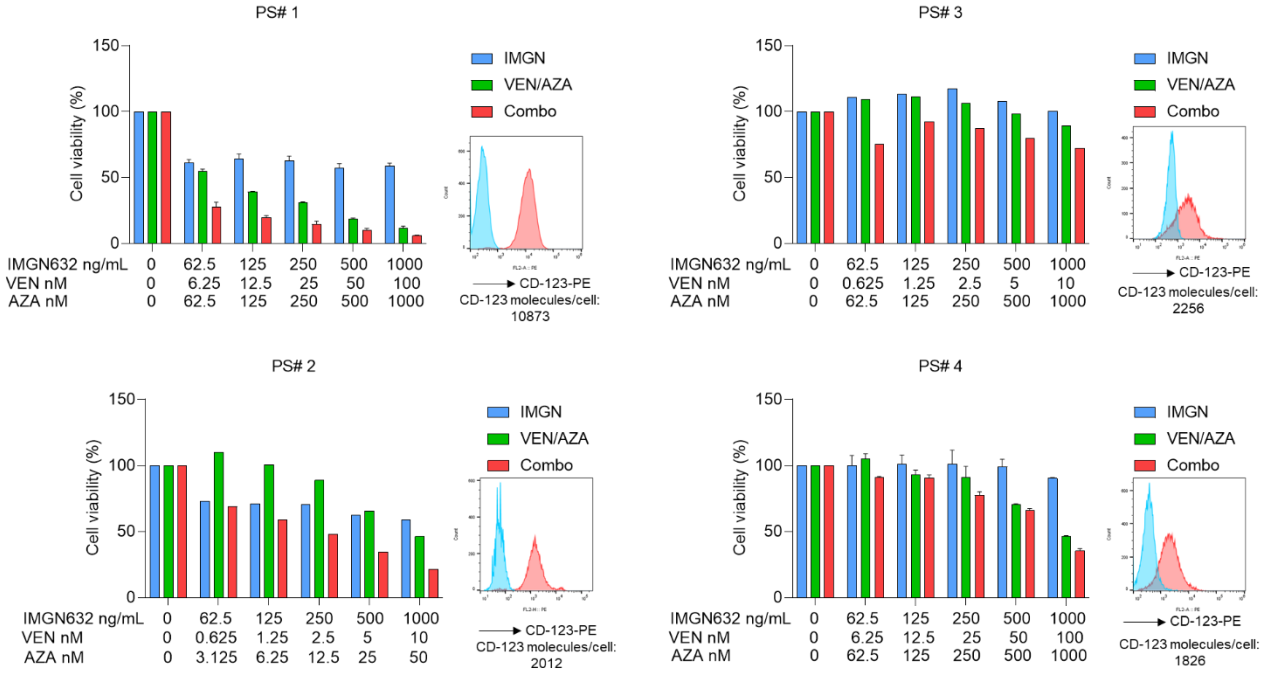

Figure 2. The effect of IMGN632/VEN/AZA combination on primary AML cells. Histograms represent flow cytometry analysis of CD-123 expression following anti-CD123-PE (red) and anti-IgG-PE (blue) staining. Number of CD-123 molecules/cell was calculated using BD Quantibrite Beads PE Fluorescence Quantitation Kit.

In the previous reporting period, we have shown that IMGN632 alone, as well as in combination with VEN/AZA, induced profound DNA damage (evidenced by increase in phosphorylated gamma-H2AX). At lower doses IMGN632 triggered cell cycle arrest either in the G1 phase (MOLM13 and MOLM14 cells) or G2/M phase (MV4-11, CAL-1 and Gen 2.2 cells) of the cell cycle. To get an insight into molecular mechanism of the observed cell cycle arrest, first we performed an EdU/PI assay which allows to determine the percentage of cells in S-phase of the cell cycle, synthesizing DNA. EdU (5-ethynyl-2'-deoxyuridine) is a terminal alkyne-containing nucleoside analog of thymidine and is incorporated into DNA during active DNA synthesis. As shown

in Figure 3, IMGN632 alone significantly decreased percentage of S-phase in AML and BPDCN cells in a dose-dependent manner.

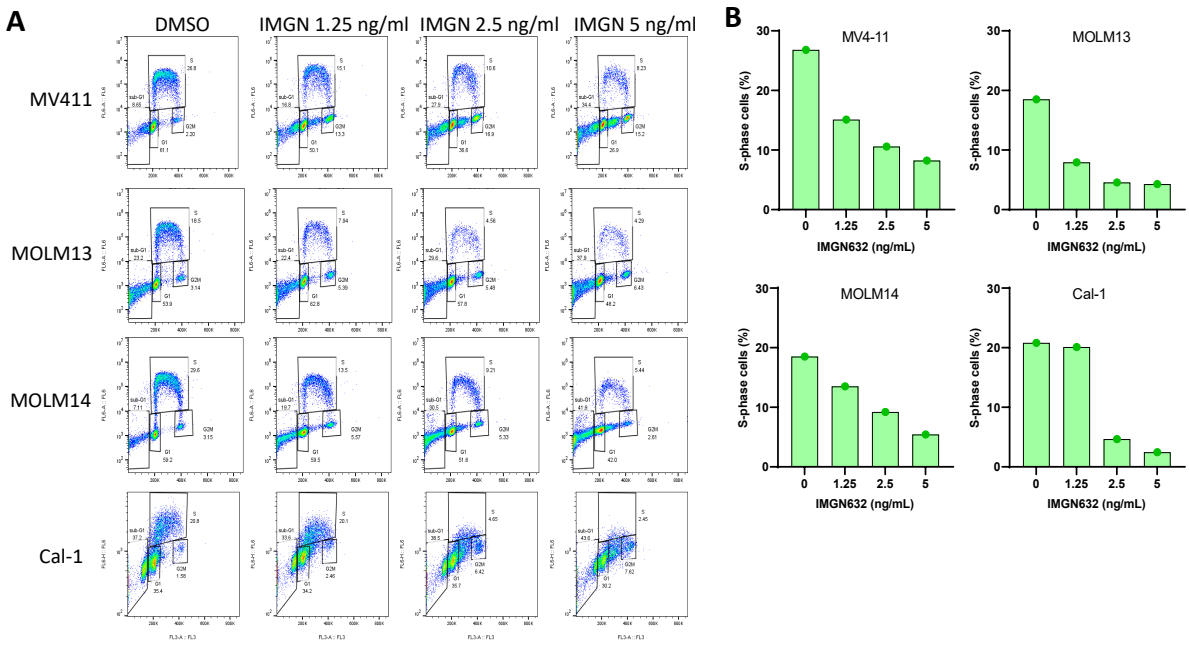

Figure 3. IMGN632 reduces progression of cells into S phase. A) Dot graphs from EdU-PI-flow cytometry analyses of control and IMGN632-treated cells for 24 h. Population of G1, S and G2/M and sub-G1 were gated. B) Quantification of cells in S-phase.

Next, we tested the effect of triple combination on the S-phase progression. Cells were treated with 2.5 ng/mL of IMGN632 alone for 24h, and 5 nM VEN/ 500 nM AZA was added for the next 24h. As shown in Figure 4, while IMGN632 profoundly decreased S-phase population in all tested cell lines, the effect of VEN alone on DNA synthesis was much more diverse with the intensity as follows: MV4-11>Cal-1>MOLM13. VEN did not affect MOLM14 S-phase cells. In contrast, AZA alone was most active in MOLM14 and Cal-1 cells but had no effect in MV4-11 and MOLM13 cells. Regardless of the cell type, dual IMGN632+VEN combination significantly decreased the percentage of cells in S-phase. This effect was further augmented in triple combination.

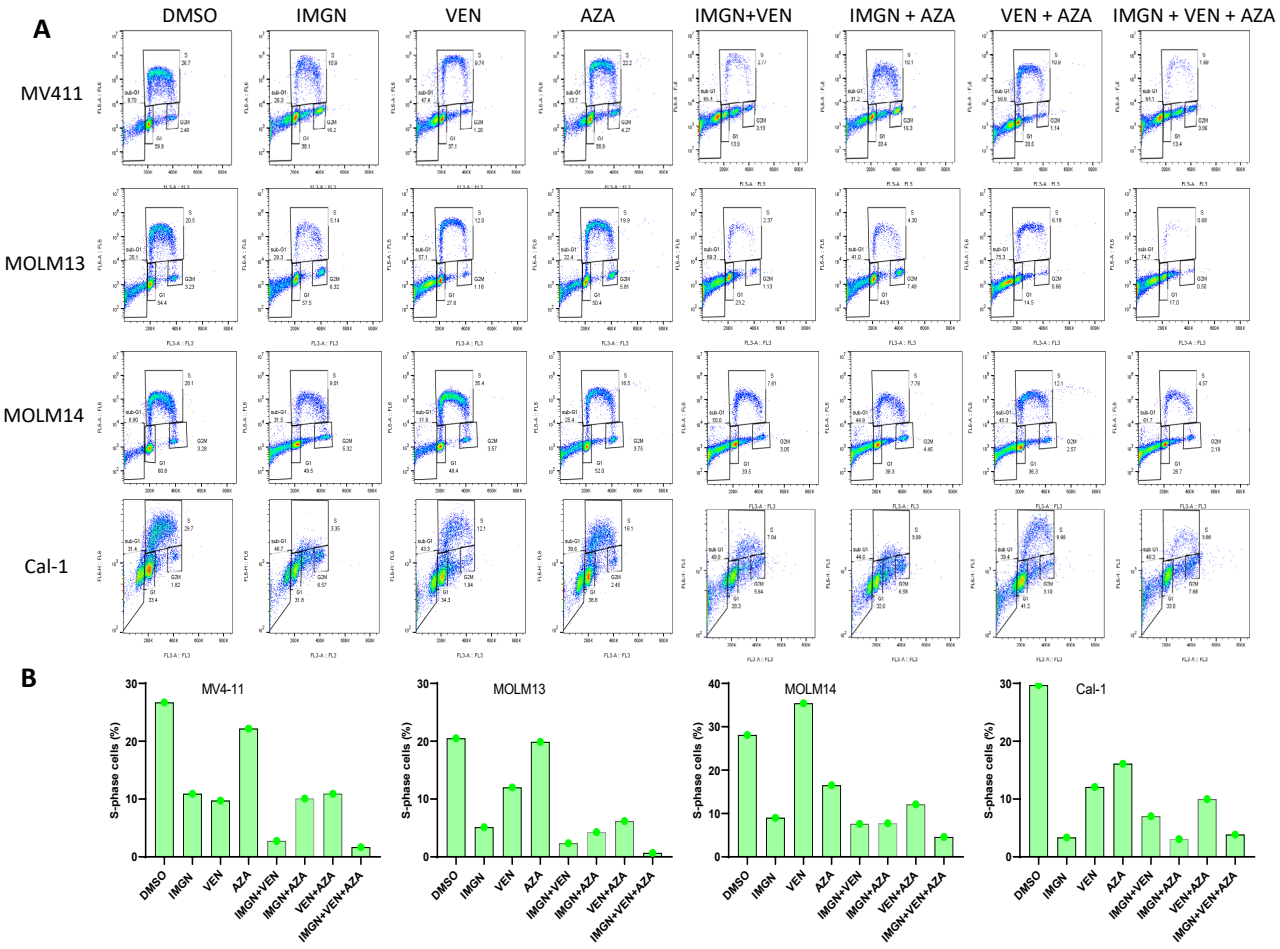

Figure 4. Triple combination of IMGN632/VEN/AZA prevents cells from entry into S-phase. Dot graphs from EdU-PI-flow cytometry analyses of cells pre-treated for 24h with 2.5 ng/mL of IMGN632, and subsequently for next 24h with 5 nM VEN and 500 nM AZA. Population of G1, S and G2/M and sub-G1 were gated. B) Quantification of cells in S-phase.

Next, we performed preliminary studies to determine whether reduced S-phase progression upon IMGN632 treatment could be due to the inability to repair DNA damage. MV4-11 AML cells were treated with 2.5 ng/mL IMGN632 for 6-48 h and subjected to western blot analysis. As shown in Figure 5, IMGN632, only after prolonged exposure (48h) significantly increased p-γH2AX level, indicative of double-strand DNA damage. This was accompanied by apoptotic caspase-3 and PARP cleavage, suggesting that observed DNA damage is a downstream event and may result from apoptosis. At the time when S-phase cells were already reduced (24h, Figure 4A and B), the level of p-γH2AX was lower than in control cells. Importantly, starting from 12 h of IMGN632 treatment there was a gradual increase in p53 phosphorylated on Ser15, indicating activation of p53 that governs cell progression through the cell cycle. Together, these results suggest that while IMGN632 may not

directly induce double-stranded DNA damage, it triggers activation of DNA-damage sensor, p53, which subsequently prevents cells from entering S-phase.

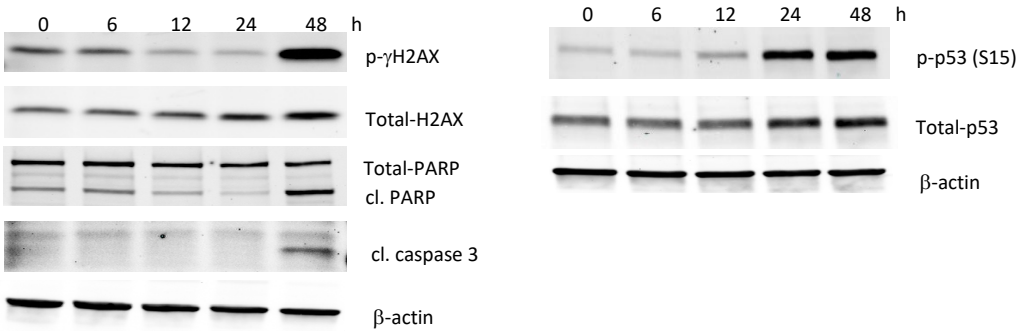

Figure 5. Western blot analysis of DNA-damage and apoptosis-associated proteins in MV4-11 cells treated with 2.5 ng/mL IMGN632 for indicated time.

Further, we performed preliminary studies to determine whether/how VEN affected IMGN632-mediated S-phase decrease. First, we pretreated MV4-11 cells with IMGN632 for 24 h and subsequently co-treated cells with VEN for 6, 16 and 24 h. S-phase progression was analyzed by flow cytometry using EdU/PI assay. As shown in Figure 6, at early time of IMGN632 and VEN co-treatment (6 h), cells were able to enter S-phase, but this process was significantly suppressed after 16 and 24 h of combined exposure. Interestingly, in comparison to IMGN632 single agent treatment, dual IMGN632+VEN combination resulted in an increase in the fraction of cells that did not synthesize DNA despite a DNA content between 2N and 4N (S non-replicating population). VEN alone did not lead to accumulation of S non-replicating cells. Prolonged exposure to IMGN+VEN also resulted in an increased frequency of apoptosis (sub-G1 population). These observations suggest that while IMGN632 alone significantly reduces cell proliferation, substantial population of cells can still proliferate. Combination of IMGN632 with VEN may help to prevent those cells from replicating DNA leading to better elimination of leukemic cells.

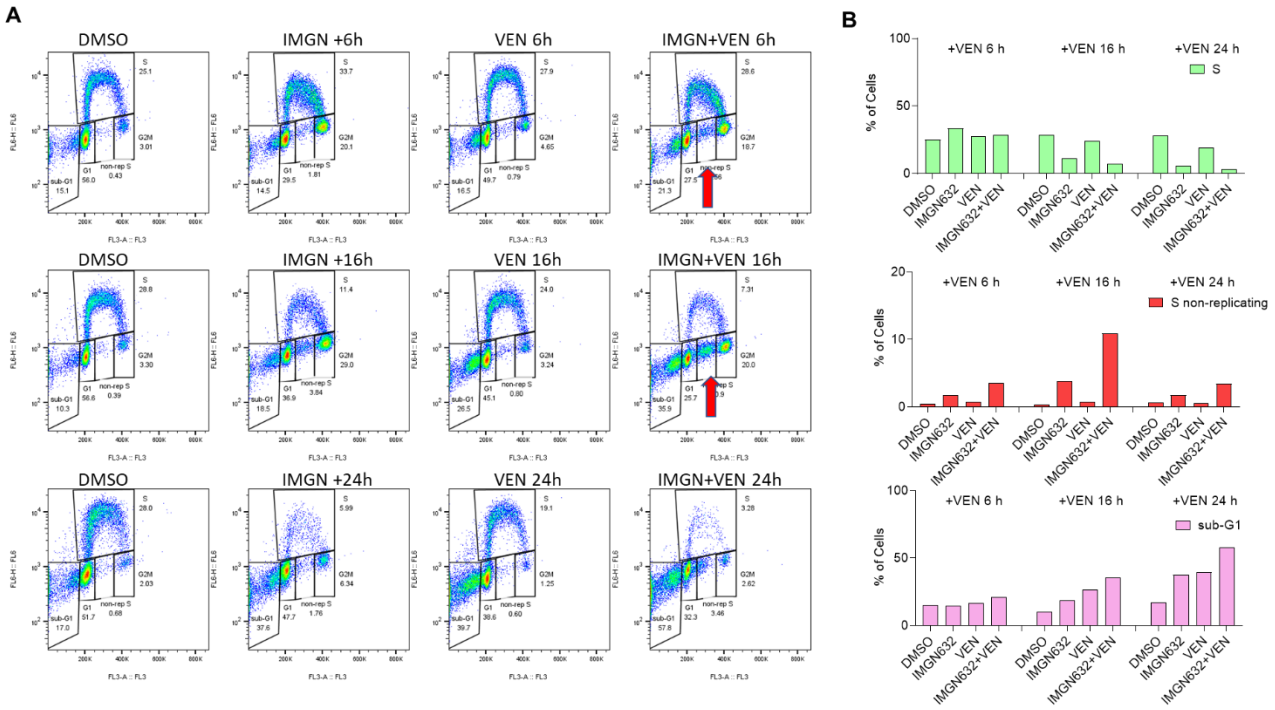

Figure 6. Effect of dual IMGN632 + VEN combination on MV4-11 cell cycle progression. A) Representative histograms from EdU-PI-flow cytometry analyses of cells pre-treated for 24h with 2.5 ng/mL of IMGN632, and subsequently for 6, 16, and next 24h with 5 nM VEN. Population of G1, S, S-non-replicating (red arrows), G2/M and sub-G1 were gated. B) Quantification of cells in S-phase, non-replicating S-phase and apoptotic sub-G1 cells.

Next, we examined whether reduced S-phase progression upon IMGN632 treatment could results from cells' inability to repair DNA damage. MV4-11 AML cells were treated with 2.5 ng/mL IMGN632 for 24 h and co-incubated with 5 nM of VEN for additional 6, 16 and 24 h, and subjected to western blot analysis. As shown in Figure 7, IMGN632, significantly increased p-γH2AX level, indicative of double-strand DNA damage. This was accompanied by increase in p53 phosphorylated on S15, indicating activation of p53 that governs cell progression through the cell cycle. In addition, IMGN632 alone increased level of phospho-Chk1 kinase, a component of ATR-Chk1 DNA damage response and DNA replication checkpoint. These results suggest that IMGN632 treatment leads to double-stranded DNA damage, which triggers activation of DNA-damage response sensors, p53 and Chk1, which subsequently prevents cells from entering S-phase. While single agent VEN treatment produced similar level of p-γH2AX, the drug neither triggered phosphorylation of p53 nor substantial phosphorylation of Chk1. Upon combined IMGN632+VEN treatment, p53 phosphorylation was sustained, but phosphorylated ChK1 decreased with time, suggesting that VEN may impair DNA damage response initially triggered by IMGN632, which in the presence of elevated DNA damage (manifested by increased by p-γH2AX), can lead to enhanced leukemia cell killing.

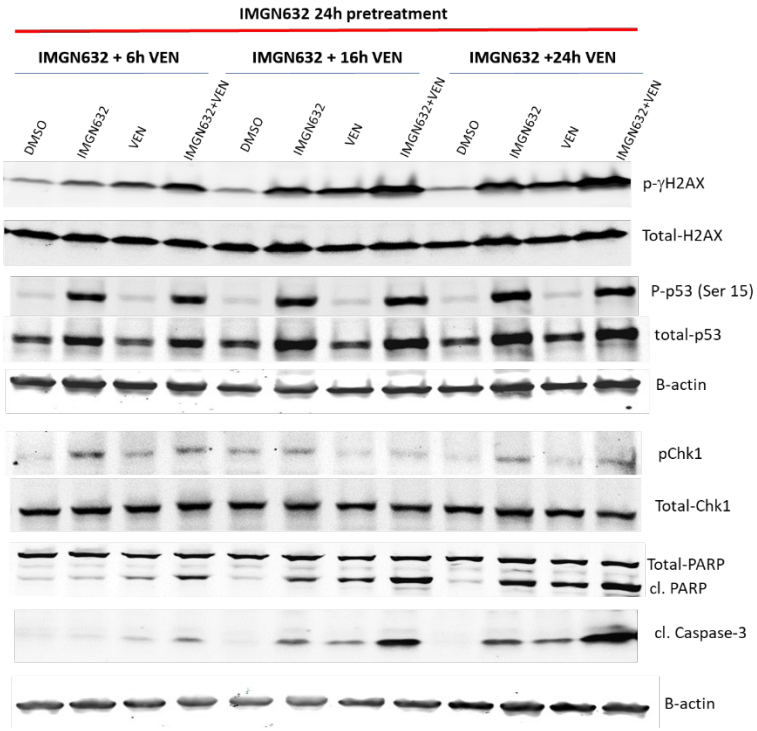

Figure 7. Western blot analysis of DNA-damage and apoptosis-associated proteins in MV4-11 cells treated with 2.5 ng/mL IMGN632 for 24 h and co-treated with 5 nM VEN for indicated times.

By using isogenic MOLM-13 p53 WT and KO cells, we have previously shown that loss of p53 profoundly reduced the potential of IMGN632/VEN/AZA combination to reduce cell growth and induce apoptosis. While most of *de novo* acute myeloid leukemia (AML) present unaltered *TP53* alleles, *TP53* mutations are frequently detected in AML related to an increased genomic instability, such as therapy-related (t-AML) or AML with myelodysplasia-related changes. Since optimal treatment strategy for patients harboring *TP53* mutations remains a critical area of unmet need, next we initiated preliminary tests of the IMGN632 activity in AML cells carrying *TP53 R284Q* and *TP53 R175H* mutations. First, cells were screened for CD-123 expression using anti-CD-123-PE and subjected to flow cytometry analysis. As shown in Figure 8A, p53-mutated cells expressed high level of CD-123, although the number of CD-123 molecules/cell was slightly lower in comparison with cells with wild-type p53. Correspondingly, the cytotoxic activity of IMGN632 although slightly lower for p53 mutants, was still within the same concentration range as for wild type p53 cells (Figure 8B).

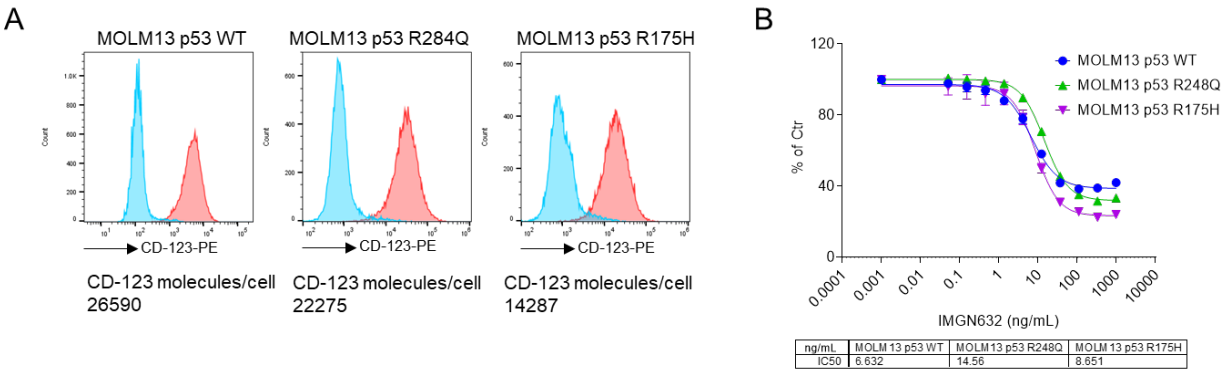

Figure 8. The effect of IMGN632 on MOLM-13 cells carrying *TP53* mutations. A) Histograms represent flow cytometry analysis of CD-123 expression following anti-CD123-PE (red) and anti-IgG-PE (blue) staining. Number of CD-123 molecules/cell was calculated using BD Quantibrite Beads PE Fluorescence Quantitation Kit. B) Cell viability was determined by CTG assay after 48 h incubation with IMGN632.

Next, we focused on determining the mechanism of synergy between IMGN632 and venetoclax. We evaluated whether IMGN632 might change AML cell dependency on BCL-2 family proteins for the survival and affect apoptotic priming. To characterize direct BCL-2 family priming following CD123 targeting, we pre-treated MV4-11 and MOLM14 cells with IMGN632 for 24 h and subjected cells to BH3 profiling. BH3 profiling determines a cell's propensity to undergo apoptosis (priming) after stimulation with pro-apoptotic peptides or drugs that mimics BH3-only proapoptotic proteins. BH3 profiling is a short-term priming assay that allowed us to measure dependence of IMGN632-treated AML cells on BCL-2, BCL-X_L or MCL-1. In our preliminary experiments apoptotic priming was measured by the relative cytochrome C release by flow cytometry for cells treated with IMGN632 compared to DMSO, followed by 1-hour treatment with venetoclax (BCL-2 priming), Navitoclax (BCL-XL priming) or S63845 (MCL-1 priming). Exposure to BIM-mimicking peptide was used as a marker of general priming for apoptosis and Alamethicin served a positive control for mitochondria depolarization. As shown in Figure 9, IMGN632 did not significantly primed cells to apoptosis. Untreated and IMGN632-treated cells released cytochrome C to the similar extent when stimulated with BIM peptide. However, the release of cytochrome C in untreated cells reached almost 100% upon exposure to 0.03 μM of BIM peptide, thus we were not able to detect a potential priming resulting from IMGN632 treatment. Further experiments with lower doses of BIM peptides are currently undergoing. Irrespectively, IMGN632-treated MV4-1 and MOLM14 cells significantly released cytochrome C in response to varied concentrations of venetoclax, indicating that IMGN632 primed AML cells to venetoclax-induced cell death and providing strong rationale for IMGN632/VEN combination. In addition, we also observed mitochondria depolarization in response to Navitoclax. These results indicate that cells sensitivity to IMGN632 may be also associated with functional BCL-XL dependence and that IMGN632 may be also effective in combination with drugs targeting BCL-XL. No priming was observed upon treatment with MCL-1 inhibitor S63845.

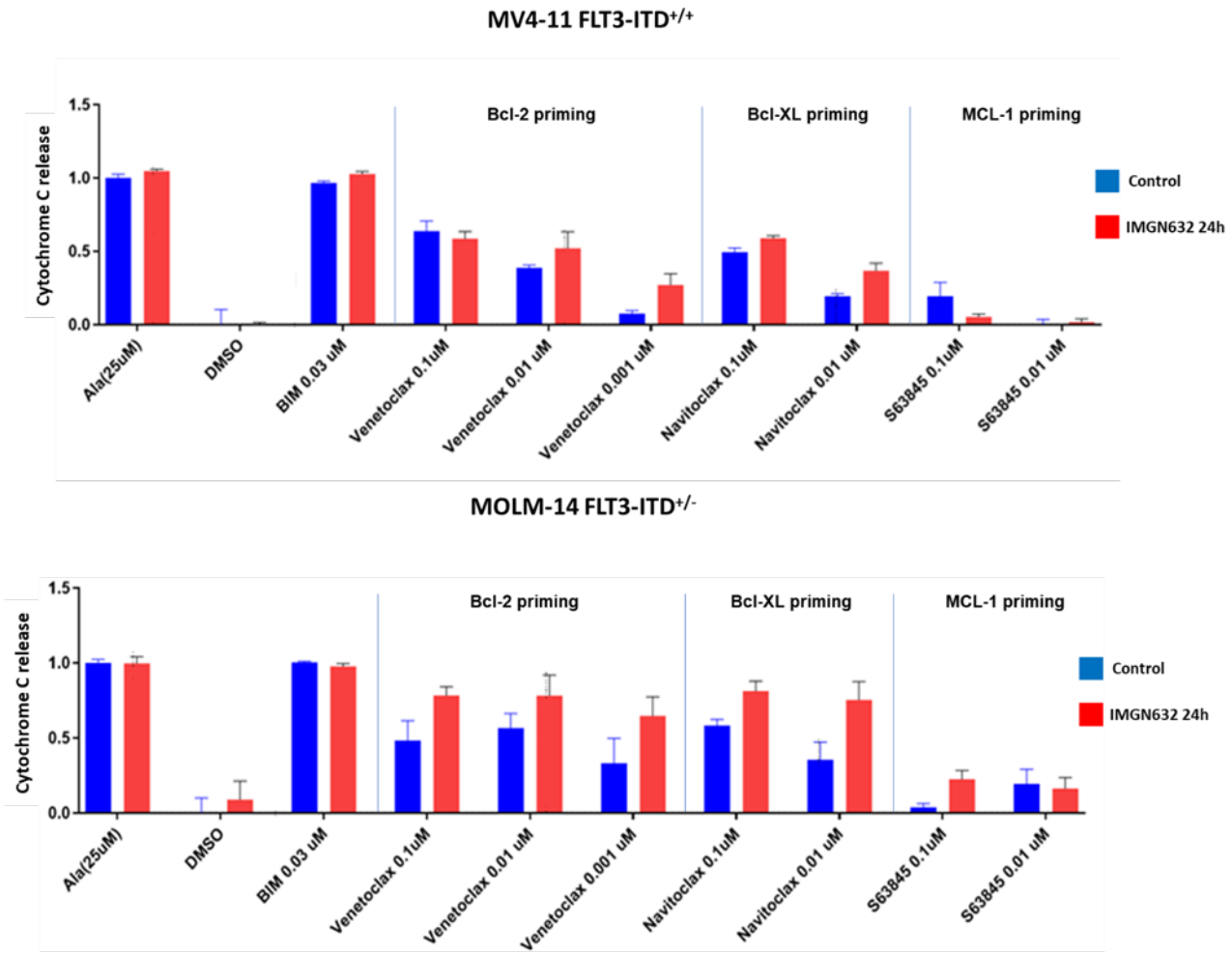

Figure 9. BH3 profiling of AML cells treated with IMGN632 for 24 h. Priming response was measured after exposure of IMGN632-treated cells to venetoclax (BCL-2 priming), Navitoclax (BCL-XL priming) or S63845 (MCL-1 priming) and expressed as a fold change in cytochrome release relative to DMSO treated control cells.

(Konopleva)
Specific Aim 2, Major Task 2: Determine the efficacy of combining anti-CD123 therapy with AZA/venetoclax in vivo.

Studies from this task were completed in 2021 and presented in the Annual Report 2021.

Specific Aim 2, Major Task 3:

The goal of this task is to obtain approval, activate, and enroll additional patients with BPDCN on a clinical trial testing the triplet combination of tagraxofusp, azacitidine, and venetoclax. We have made good progress on this task during the funding period. Our SOW goal was to open the trial to enrollment in Year 2. During the prior funding period, the clinical trial testing TAG/AZA or TAG/AZA/VEN for patients with acute myeloid leukemia (AML) or myelodysplastic syndrome (MDS) completed dose escalation and the recommended phase 2 dose (RP2D) was determined for the TAG/AZA/VEN triplet. This allowed us to open the expansion cohorts for patients with BPDCN using the RPD2 of TAG/AZA/VEN, which is AZAcitidine 75 mg/m2 on days 1-7, VENetoclax 400 mg daily on days 1-21, and TAG 12 ug/kg/day on days 4-6.

We opened two arms for patients with BPDCN, one for first line treatment and one for relapsed or refractory BPDCN. To date, 6 patients with r/r BPDCN have been enrolled and one patient with previously untreated BPDCN has been enrolled. Correlative samples are being collected from all patients for future laboratory analysis. The analysis is ongoing, but we are seeing encouraging results. These include that there is no obvious difference in adverse events between patients with BPDCN and the prior dose-finding cohorts of patients with AML. Second, we have seen complete responses (CRs) in 4 of 6 patients with r/r BPDCN. All four had received prior single agent TAGraxofusp, which is very encouraging for our mechanistic hypothesis for overcoming TAG resistance. All four also proceeded to stem cell transplantation, which is always our goal for patients with BPDCN. Overall, we are very pleased with our progress and we continue to enroll subjects with BPDCN.

Aim 3 – Abdel-Wahab

Major Task 2: Determine aberrant splicing events generated by mutant *ZRSR2* and *SRSF2* in BPDCN which promote transformation through a positive enrichment CRISPR screen. The progress we have made is as follows:

Mapping direct RNA binding targets of ZRSR2: To understand the mechanistic basis for the relationship between ZRSR2 mutations in BPDCN and alterations in splicing of minor introns, we attempted to identify direct binding targets of ZRSR2 on RNA. We therefore performed anti-ZRSR2 eCLIP-seq[31] (enhanced UV crosslinking immunoprecipitation followed by next-generation sequencing) in human myeloid leukemia (K562) cells (**Fig. 10A**). This revealed that ~80% of ZRSR2 binding sites mapped to exons, with a highly significant enrichment for ZRSR2 binding to minor intron-containing genes whose minor intron was responsive versus non-responsive to *ZRSR2* mutations (**Fig. 10A-B**; p-value < $2.2e^{-16}$ with an odds ratio in the range (95% CI): 2.1-2.5). ZRSR2 binding was specifically enriched in minor introns, consistent with our analyses of the effects of ZRSR2 loss on minor intron retention (**Fig. 10C**). Finally, ZRSR2-bound mRNAs are enriched for mRNAs encoding RNA regulatory proteins as well as genes with known involvement in leukemia and protein processing and translation (**Fig. 10D**). Overall, these analyses identify that minor intron-containing genes whose splicing is regulated by ZRSR2 are direct binding targets of ZRSR2.

Both the RNA-seq and eCLIP-seq analyses above identified that only approximately one-third of U12-type intron-containing genes are sensitive to loss of ZRSR2. In order to understand the specificity of ZRSR2 for regulation of the splicing of minor introns and why only a portion of minor introns are regulated by ZRSR2, we next evaluated the sequence features of introns which were retained upon ZRSR2 loss.

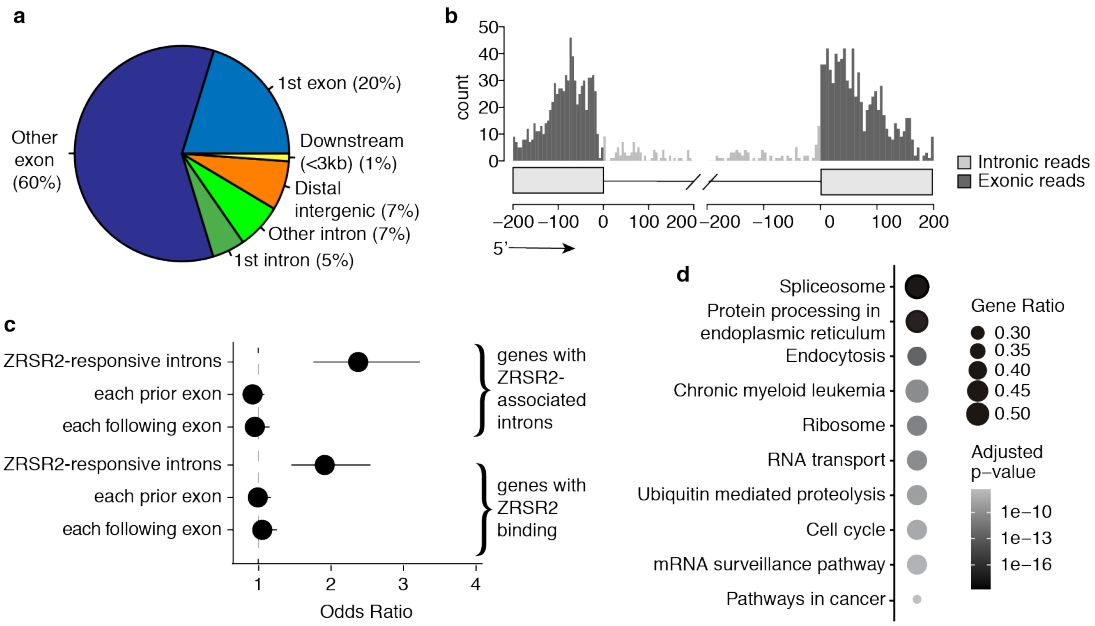

Figure 10. ZRSR2 RNA binding targets. (a) Genomic distribution of ZRSR2 eCLIP-seq (enhanced UV crosslinking immunoprecipitation followed by next-generation sequencing) peaks. **(b)** Metaplot of ZRSR2 eCLIP sequencing reads at ZRSR2-regulated minor introns. **(c)** Fisher's exact test analysis evaluating the enrichment of ZRSR2 within responsive introns and each flanking exon by eCLIP-seq in genes with ZRSR2-responsive introns or those with ZRSR2 binding. **(d)** Gene ontology analysis of ZRSR2-bound genes by eCLIP-seq.

Characteristics of ZRSR2 regulated introns: While branchpoints within U2-type introns are highly constrained in their location, branchpoints within U12-type introns exhibit a bimodal distribution, such that half of U12-type introns have branchpoints similar in location to U2-type branchpoints while half of U12-type branchpoints occur in closer proximity (within 20 nucleotides (nt)) of the 3' splice site (3'ss)[32] (**Fig. 11A**). To test whether this bimodality was relevant to ZRSR2 responsiveness, we augmented our previously published branchpoint annotation by querying available RNA-seq data from cohorts within The Cancer Genome Atlas (TCGA) to search for lariat-derived reads which span the 5' splice site-branchpoint junction within minor introns. Such reads are extremely rare due to typically rapid lariat degradation—hence the need for an extremely large-scale analysis—but allow for inference of branchpoint location with nucleotide-level resolution. Using this large U12-type branchpoint annotation, we discovered that introns that respond to ZRSR2 loss had branchpoints that were significantly more proximal to the 3'ss than did non-responsive introns (two-sided Kolmogorov-Smirnov test $p<2.2e-16$; **Fig. 11B**). In contrast, non-responsive U12-type introns exhibited no such spatially restricted enrichment, suggesting that branchpoint location influences U12-type intron susceptibility to retention in the absence of ZRSR2[32]. We therefore examined the branchpoint more closely as a potential determinant of response to ZRSR2 loss. This revealed that ZRSR2-responsive introns prefer adenosine nucleotides as branchpoints (**Fig. 11C**; $p=1.5x10^{-5}$ by two-sided binomial proportion test); have more branchpoints per intron compared to ZRSR2 non-responsive introns (**Fig. 11D**; $p=0.03$ by two-sided *t*-test); and have branchpoints that more closely match the U12 snRNA consensus sequence (**Fig. 11E**; $p=5.2e10^{-16}$ by Wilcoxon rank sum test). ZRSR2-responsive minor introns additionally have less-defined polypyrimidine tracts and a reduced preference for G at the +1 position compared to

non-responsive introns (**Fig. 11F-G**). Overall, these data identify that U12-type introns fall into two classes: those which are resistant to ZRSR2 loss and those which respond strongly to ZRSR2 loss. Responsive introns are typically characterized by a 3'ss-proximal, adenosine branchpoint that is surrounded by nucleotides that closely resemble the U12 snRNA consensus, as well as having a weak or absent polypyrimidine tract.

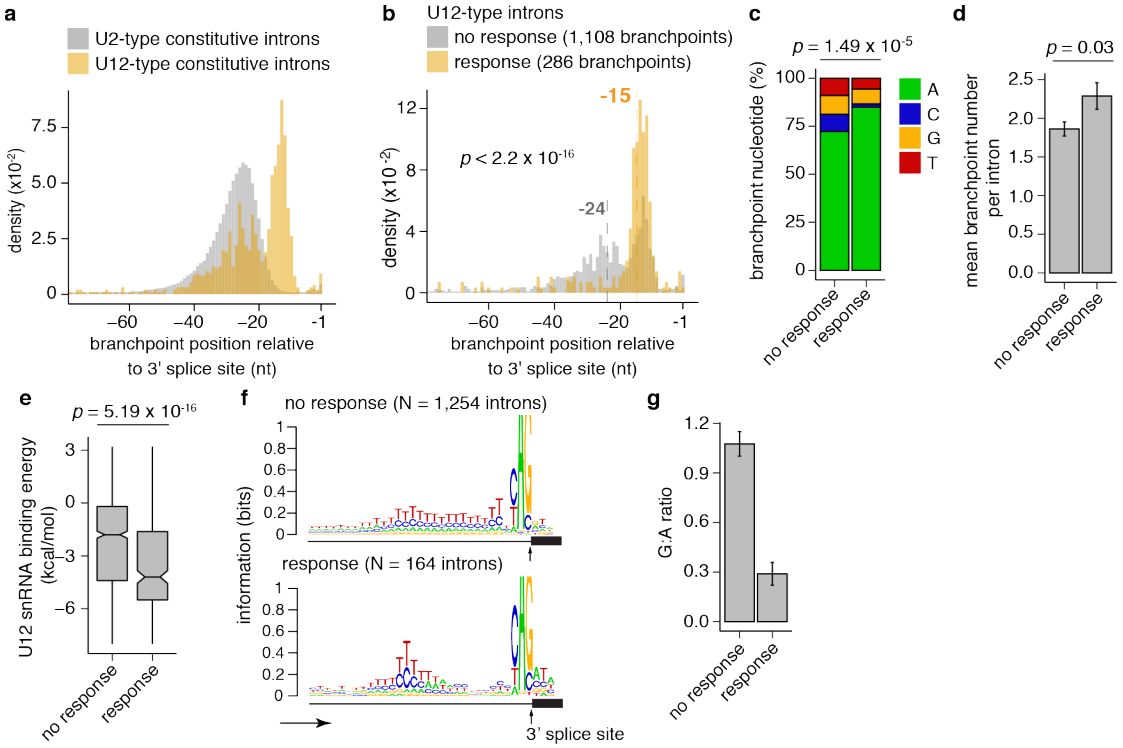

Figure 11. Features of ZRSR2-responsive introns (a) Histogram of the locations of branchpoints relative to the 3' splice site (3'ss) in U2- versus U12-type constitutive introns. **(b)** Histogram of the locations of branchpoints relative to the 3'ss for ZRSR2 non-responsive versus responsive minor introns (*p*-value estimated by a two-sided Kolmogorov-Smirnov test). **(c)** Branchpoint nucleotide preference for ZRSR2 non-responsive versus responsive minor introns (*p*-value estimated with a two-sided binomial proportion test for a difference in fraction of adenine branchpoints). **(d)** Mean number of branchpoints within ZRSR2 non-responsive versus responsive minor introns (*p*-value estimated by a two-sided *t*-test). Error bars represent $\pm$ 1 standard error of the mean (sd/sqrt(n)). **(e)** U12 snRNA binding energy for branchpoint motifs in ZRSR2 non-responsive versus responsive minor introns (*p*-value estimated by a two-sided Mann-Whitney *U* test). **(f)** Sequence logo plots of the 3'ss of ZRSR2-responsive versus non-responsive introns (upward arrow indicates site of 3'ss). As shown, ZRSR2-responsive introns have weaker/less-defined polypyrimidine tracts. **(g)** G:A ratio at the +1 position (relative to the 3'ss). Error bars represent $\pm$ 1 s.d. estimated by bootstrapping (10k iterations). P-value = 0 by two-sided Mann-Whitney U test.

Aim 3, Major Task 2: **Determine aberrant splicing events in BPDCN through CRISPR screening.** As noted in our prior progress report, we performed genome-wide CRISPR/Cas9 screens to identify drug-gene interactions that modulate therapeutic response to treatments commonly used in AML and BPDCN. Interestingly, our findings uncovered several genes that regulate pre-mRNA splicing whose loss strongly synergized with venetoclax. This effort eventually led us to develop and evaluate a novel compound (in collaboration with Bio-Splice Therapeutics) which perturbs RNA splicing via inhibition of CLK kinases CLK1-4 as well as DYRK kinases DYRK1A, DYRK1B, and DYRK2. CLKs phosphorylate Arginine-Serine (RS) domains in SR proteins and regulate pre-mRNA splicing. Moreover, DYRK1A has been reported to regulate alternative splicing via phosphorylation

of SF3B1. In addition, analysis of publicly available genome wide CRISPR screens from DepMap revealed BCL2 as one of the top co-dependencies with DYRK1A loss.

These findings supported the rationale to evaluate inhibition of splicing-dependent kinases as a combinatorial strategy with venetoclax. To pursue therapeutic inhibition of splicing-dependent kinases, in collaboration with Bio-Splice we developed SM09419, a small molecule 3-acylamino-isoquinoline analog that was rationally designed and optimized through iterative medicinal chemistry to achieve drug-like and favorable pharmacokinetic profiles (**Fig. 12A-B**). Accordingly, SM09419 treatment resulted in dose-dependent reduction of CLK activity and SR protein phosphorylation in AML cells. We observed a synergistic effect in combining SM09419 and venetoclax when compared to single-agent activity in human AML cell lines.

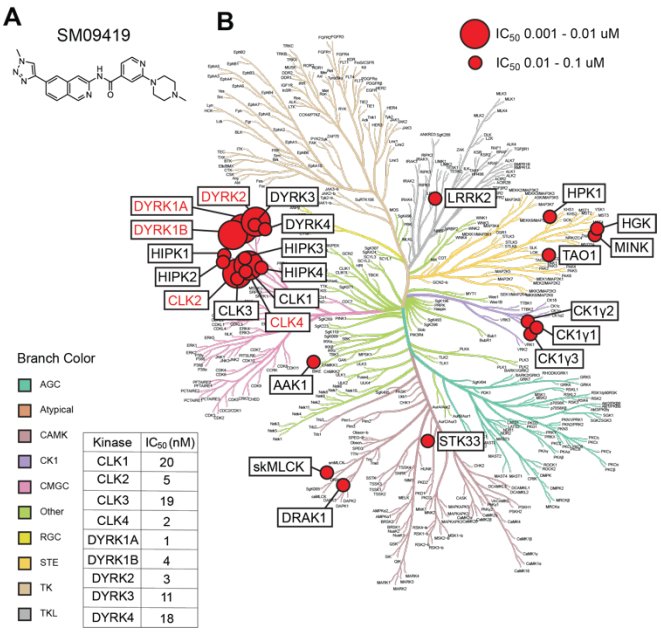

Kinase	IC_{50} (nM)
CLK1	20
CLK2	5
CLK3	19
CLK4	2
DYRK1A	1
DYRK1B	4
DYRK2	3
DYRK3	11
DYRK4	18

Fig. 12. Development of plan-CLK/DYRK inhibitor SM09419. (A) Structure of SM09419. **(B)** Kinase dendrogram of SM09419 specificity. Kinases with IC50 values of 0.01 to 0.1μM are indicated by small red circle, whereas larger red circles represent more potent IC50 values of 0.001 to 0.01μM.

To understand the mechanistic basis for the preferential synergy of SM09419 and venetoclax combination, we performed RNA-seq on MOLM-13 human AML cells treated with SM09419 alone or in combination with venetoclax. Transcriptomic analysis of SM09419-treated AML cells demonstrated downregulation of MYB and MYC mRNA levels, which are essential oncogenic programs in AML. Splicing analyses showed that SM09419 alone, or in combination with venetoclax, mainly resulted in changes in the processing of constitutive/retained introns and cassette exons. CLK/DYRK inhibition affects cassette exon recognition in a sequence-specific manner, as evidenced by the enrichment of pyrimidines in exons preferentially excluded upon SM09419 treatment (**Fig. 13A**). While venetoclax monotherapy had no significant effects on RNA splicing, treatment with SM09419 or the combination resulted in striking reductions in RNA splicing efficiency as manifested by cassette exon skipping (n=1,473) and intron

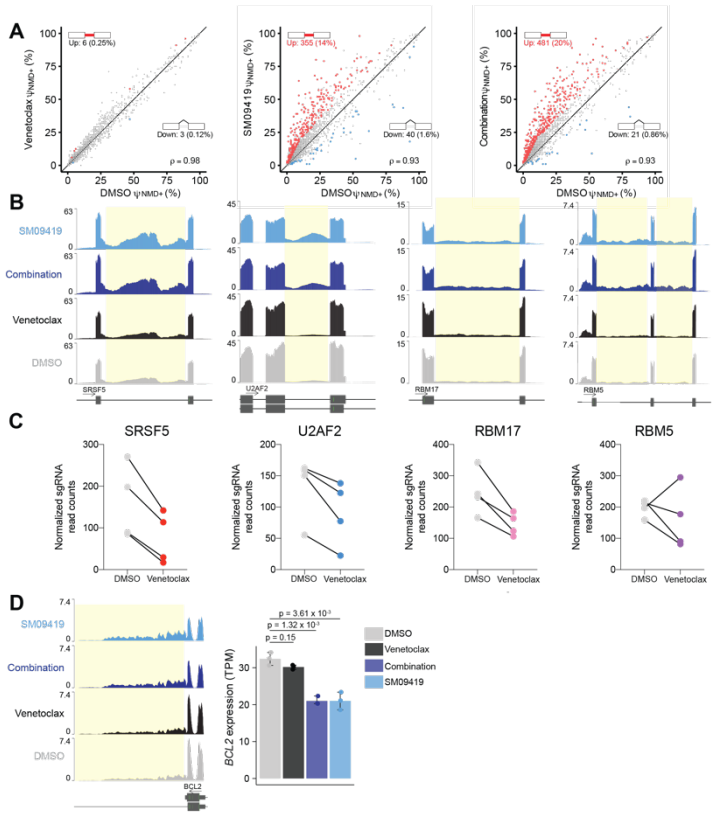

Fig. 13. SM09419 promotes mis-splicing of key oncogenic pathways in AML. (A) Scatter plot of NMD-inducing retained intron (RI) events (red circles) in MOLM-13 cells treated with venetoclax (left), SM09419 (middle) or the combination of venetoclax and SM09419 (right). **(B)** RNA-seq coverage plots of the splicing factors, SRSF5, U2AF2, RBM17, RBM5 in MOLM-13 cells. Yellow re-gions represent retained intron events in each of the genes. **(C)** Normalized sgRNA counts of top splicing fac-tors from RNA-binding protein CRISPR screen that synergized with venetoclax treatment in MOLM-13 cells. **(D)** RNA-seq coverage plots (left) and gene expression (right) for BCL2 mRNA (left). P-values determined by two-sided t-test

retention (n=395) (**Fig. 8A**). Of note, these splicing shifts resulted in substantial increases in levels of mRNAs that contain premature termination codons and are therefore predicted substrates for degradation by nonsense-mediated decay (NMD).

Further characterization of SM09419-associated splicing changes revealed increased intron retention within the transcripts of a number of RNA splicing factors (*SRSF5*, *U2AF2*, *RBM17* and *RBM5*) (**Fig. 13B**). Interestingly, several of these same splicing factors were also identified by our CRISPR screens as genes whose inactivation enhanced venetoclax efficacy (**Fig. 13C**). Furthermore, we identified a long intron within BCL2 that was significantly more retained upon SM09419 treatment, an event associated with downregulated BCL2 expression (**Fig. 13D**). Overall, these data identify that SM09149 downregulates expression of key RNA splicing factors as well as BCL2 via impaired RNA splicing to enhance response to venetoclax in AML cells while having minimal impact on normal hematopoietic cells.

SM09419 treatment demonstrated approximately equally potent inhibitory activity against venetoclax-resistant AML cells as parental, venetoclax sensitive cells. We further extended these findings to patient-derived xenograft (PDX) models of AML from patients with *de novo* resistance to venetoclax combination regimens (5-azacytidine or low-dose cytarabine) (**Fig. 14A**). Following xenotransplantation from two individual venetoclax-resistant patients into NSGS mice, we detected disease engraftment with ≥10% human $hCD45^+$ $hCD34^+$ $hCD38^+$ cells and exposed mice to SM09419 (25 mg/kg) or vehicle administered orally for 3 weeks. SM09419 resulted in significant reduction of hCD45 AML cells in the peripheral blood and bone marrow of mice treated with SM09419 when compared to vehicle control (**Fig. 14B-D**). Collectively, these findings demonstrate the potent single agent *in vivo* efficacy of SM09419 to overcome resistance to venetoclax-based therapies.

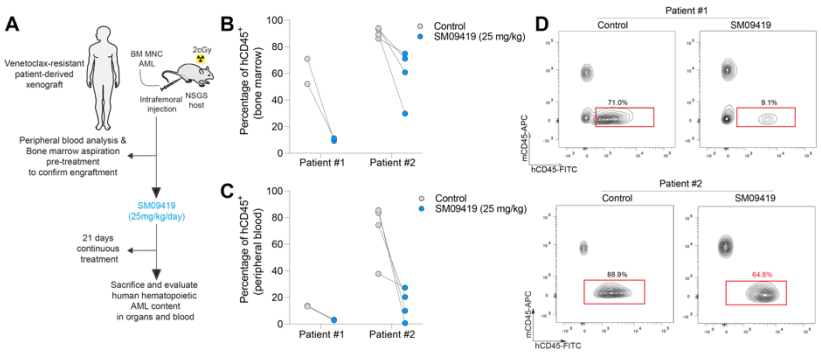

Fig. 14. SM09419 circumvents therapeutic resistance to venetoclax. (A) Schematic of patient-derived xenograft (PDXs) generation and treatment with SM09419 (25 mg/kg, QD, PO) or vehicle. **(B)** Percentage of human CD45+ (hCD45+) cells in bone marrow and **(C)** peripheral blood of PDXs following 3-weeks of SM09419 treatment. **(D)** Representative flow-cytometry plots of hCD45+ and mouse CD45+ (mCD45+) in bone marrow from PDXs treated with 25 mg/kg SM09419 after 3-weeks.

What opportunities for training and professional development has the project provided?

Nothing to report

How were the results disseminated to communities of interest?

(Konopleva)
<u>We have presented following posters at the national meetings:</u>
2020 ASH
Combining IMGN632, a Novel CD123-Targeting Antibody Drug Conjugate with Azacitidine and Venetoclax Facilitates Apoptosis *in Vitro* and Prolongs Survival *In Vivo* in AML Models
https://www.sciencedirect.com/science/article/pii/S0006497118720326

2020 SOHO
AML-367: IMGN632, a CD123-Targeting ADC Bearing a DNA-Alkylating IGN Payload, Combines Effectively as a Triplet Regimen with Azacitidine and Venetoclax In Vivo, Prolonging Survival in Preclinical Models of Human Acute Myeloid Leukemia (AML)
https://www.sciencedirect.com/science/article/pii/S2152265020307680

2019 ASH
IMGN632, a CD123-Alkylating ADC Bearing a DNA Alkylating IGN Payload, Combines Effectively with Azacitidine and Venetoclax In Vivo, Prolonging Survival in Preclinical Models of Human Acute Myeloid Leukemia (AML)
https://ashpublications.org/blood/article/134/Supplement_1/1375/427254/IMGN632-a-CD123-Alkylating-ADC-Bearing-a-DNA

2019 EHA
PF201 THE COMBINATION OF IMGN632, A CD123-TARGETING ADC, WITH VENETOCLAX ENHANCES ANTI-LEUKEMIC ACTIVITY IN VITRO AND PROLONGS SURVIVAL IN VIVO IN PRE-CLINICAL MODELS OF HUMAN AML
https://journals.lww.com/hemasphere/Abstract/2019/06001/PF201_THE_COMBINATION_OF_IMGN632,_A.101.aspx

2018 ASH
Pre-Clinical Efficacy of CD123-Targeting Antibody-Drug Conjugate IMGN632 in Blastic Plasmacytoid Dentritic Cell Neoplasm (BPDCN) Models
https://www.sciencedirect.com/science/article/pii/S0006497119400566

(Lane)
Conference abstract oral presentation:

Togami K, Chung SS, Madan V, Kenyon CM, Cabal-Hierro L, Taylor J, Kim SS, Griffin GK, Ghandi M, Li J, Li YY, Angelot-Delettre F, Biichle S, Seiler M, Buonamici S, Lovitch SB, Louissaint A, Moran EA, Jardin F, Piccaluga PP, Weinstock DM, Hammerman PS, Yang H, Konopleva M, Pemmaraju N, Garnache-Ottou F, Abdel-Wahab O, Koeffler P, Lane AA. Male-Biased Spliceosome Mutations in Blastic Plasmacytoid Dendritic Cell Neoplasm (BPDCN) Impair pDC Activation and Apoptosis. Oral presentation. American Society of Hematology Annual Meeting 2020. *Blood* (2020) 136 (Supplement 1): 13–14. https://doi.org/10.1182/blood-2020-137727

(Lane)
Published paper:

Togami K, Chung SS, Madan V, Booth CAG, Kenyon CM, Cabal-Hierro L, Taylor J, Kim SS, Griffin GK, Ghandi M, Li J, Li YY, Angelot-Delettre F, Biichle S, Seiler M, Buonamici S, Lovitch SB, Louissaint A, Moran EA, Jardin F, Piccaluga PP, Weinstock DM, Hammerman PS, Yang H, Konopleva M, Pemmaraju N, Garnache-Ottou F, Abdel-Wahab O, Koeffler P, Lane AA. Sex-biased *ZRSR2* mutations in myeloid malignancies impair plasmacytoid dendritic cell activation and apoptosis. Cancer Discovery. 2022 Feb;12(2):522-541. doi: 10.1158/2159-8290.CD-20-1513. PMID: 34615655

(Abdel-Wahab)
Conference abstract oral presentation:
2020 ASH
ZRSR2 Mutation Induced Minor Intron Retention Drives MDS and Diverse Cancer Predisposition Via Aberrant Splicing of *LZTR1*

https://ash.confex.com/ash/2020/webprogram/Paper136445.html

2021 ASH
Modulation of RNA Splicing Enhances Response to BCL2 Inhibition in Acute Myeloid Leukemia
https://ashpublications.org/blood/article/138/Supplement%201/507/479370/Modulation-of-RNA-Splicing-Enhances-Response-to?searchresult=1

What do you plan to do during the next reporting period to accomplish the goals?

Aim 1 (Lane):

- We will continue to analyze eCLIP-seq data for KHSRP in BPDCN cells. The sequencing has now been completed and we are working with our bioinformatics colleagues to analyze the data to determine which RNAs are bound by KHSRP. We performed the experiment in the presence and absence of treatment and with and without KHSRP knockdown as controls, so we will also determine if drug treatment and/or the residual disease state changes the RNA binding partners of KHSRP.

- We will perform an integrated RNA-seq in BPDCN cells with and without KHSRP knockdown. We completed RNA sequencing and now are working to integrate RNA binding with dynamic gene expression differences during treatment with different inducers of targeted BPDCN cell death. This will help us understand how it protects BPDCN MRD cells after VEN/AZA and TAG from cell death.

- We have now expanded our in vivo BPDCN PDX models, and we will work to optimizing primary cell KHSRP knockdown in the context of VEN/AZA and SL401 treatments to provide validation data in primary cells. These will also form the platform for future testing of small molecule modulators that may function via the same pathway and therefore similarly sensitize BPDCN cells to the same treatments and be more amenable to short-term preclinical development. We are specifically testing the contribution of Vitamin C transporters to the sensitivity of BPDCN cells to KHSRP-loss sensitization based on preliminary synergy data with VEN/AZA and or tagraxofusp treatment.

(Konopleva)
Aim 2, Sub-Aim 1:
- Continue with studies on the mechanisms of synergistic activity of IMGN632/VEN/AZA combination in BPDCN and AML cell lines. In particular: 1) validate western blot results and expand studies on the effect of IMGN632/VEN/AZA treatment on activation of DNA damage response (DDR) pathways by confocal microscopy analysis of RAD51 foci (marker of homologous recombination, HR), 53BP1 foci (marker of non-homologous end joining, NHEJ); 2) extend western blot analysis of DDR markers: ATM/pATM(Ser1981)/CHK2/pCHK(Thr68), ATR/pATR

(Ser428)/CHK1/pCHK1 (Ser345), BRCA1/2, PARP1, p53 effectors like p21; 3) analyze the effect of venetoclax on the repair of DNA damage induced by IMGN632 by using Comet Assay; 4) expand BH3 profiling of IMGN632-primed cells by incorporating BH3 mimetic peptides to obtain better view on the cell's BCL-2 family dependencies.
- Continue studies on the role of p53 in the overall response of AML cells to IMGN632/VEN/AZA combination. In particular: test the effect of combination on the DDR and cell cycle in p53 wild-type and p53 KD AML cells.

Aim 2, Sub-Aim 3:
- We will continue to enroll patients with BPDCN to the frontline and relapsed/refractory cohorts. Samples for laboratory correlative analyses

Aim 3,(Abdel-Wahab):

Aim 3, Sub-Aim 1:
- Continue to determine the effects of perturbing splicing *in vivo* in BPDCN PDX models wild-type or mutant for RNA splicing factors.
- Continue to determine the effects of various drugs perturbing RNA splicing on splicing and gene expression in the above BPDCN models.

Aim 3, Sub-Aim 2:
- Evaluation of molecular basis for the individual splicing events found in screen as well as analysis of effects on protein expression in BPDCN samples.

4. IMPACT:

What was the impact on the development of the principal discipline(s) of the project?
Nothing to Report

What was the impact on other disciplines?
Nothing to Report

What was the impact on technology transfer?
Nothing to Report

What was the impact on society beyond science and technology?
Nothing to Report

Changes in approach and reasons for change
Nothing to Report

Actual or anticipated problems or delays and actions or plans to resolve them
Nothing to Report

Changes that had a significant impact on expenditures
Nothing to Report

Significant changes in use or care of human subjects, vertebrate animals, biohazards, and/or select agents
Nothing to Report

Significant changes in use or care of human subjects
Nothing to Report

Significant changes in use or care of vertebrate animals
Nothing to Report

Significant changes in use of biohazards and/or select agents
Nothing to Report

5. PRODUCTS:

- **Publications, conference papers, and presentations**
  Journal publications.

Conference abstract oral presentation (Lane):

Togami K, Chung SS, Madan V, Kenyon CM, Cabal-Hierro L, Taylor J, Kim SS, Griffin GK, Ghandi M, Li J, Li YY, Angelot-Delettre F, Biichle S, Seiler M, Buonamici S, Lovitch SB, Louissaint A, Moran EA, Jardin F, Piccaluga PP, Weinstock DM, Hammerman PS, Yang H, Konopleva M, Pemmaraju N, Garnache-Ottou F, Abdel-Wahab O, Koeffler P, Lane AA. Male-Biased Spliceosome Mutations in Blastic Plasmacytoid Dendritic Cell Neoplasm (BPDCN) Impair pDC Activation and Apoptosis. Oral presentation. American Society of Hematology Annual Meeting 2020. *Blood* (2020) 136 (Supplement 1): 13–14. https://doi.org/10.1182/blood-2020-137727

Published paper (Lane):

Togami K, Chung SS, Madan V, Booth CAG, Kenyon CM, Cabal-Hierro L, Taylor J, Kim SS, Griffin GK, Ghandi M, Li J, Li YY, Angelot-Delettre F, Biichle S, Seiler M, Buonamici S, Lovitch SB, Louissaint A, Moran EA, Jardin F, Piccaluga PP, Weinstock DM, Hammerman PS, Yang H, Konopleva M, Pemmaraju N, Garnache-Ottou F, Abdel-Wahab O, Koeffler P, Lane AA. Sex-biased *ZRSR2* mutations in myeloid malignancies impair plasmacytoid dendritic cell activation and apoptosis. Cancer Discovery. 2021; doi: 0.1158/2159-8290. CD-20-1513. Online ahead of print. PMID: 34615655

Acknowledgement of federal support: Yes

Books or other non-periodical, one-time publications.
Nothing to Report

Other publications, conference papers and presentations.
Nothing to Report

- **Website(s) or other Internet site(s)**
  Nothing to Report

- **Technologies or techniques**
  Nothing to Report

- **Inventions, patent applications, and/or licenses**
  Nothing to Report

- **Other Products**
  Nothing to Report

6. PARTICIPANTS & OTHER COLLABORATING ORGANIZATIONS

What individuals have worked on the project?

DFCI

Name: Andrew Lane, MD, PhD
Project Role: Site PI (DFCI)
Researcher Identifier (e.g. ORCID ID):
Nearest person month worked: 0.78 person-months per year
Contribution to Project: Dr. Lane supervised the project and worked on development and regulatory items for the clinical protocol.

Name: Qingyu Luo, PhD
Project Role: Postdoctoral fellow
Researcher Identifier (e.g. ORCID ID):
Nearest person month worked: 4.8 person-months per year
Contribution to Project: Dr. Luo analyzed the CRISPRi screen and performed initial validation work on sgRNA hits. He also performed the in vivo PDX treatment experiments with BPDCNs.

Name: Siobhan Rice, PhD
Project Role: Postdoctoral fellow
Researcher Identifier (e.g. ORCID ID):
Nearest person month worked: 6 person-months per year
Contribution to Project: Dr. Rice worked to optimize CRISPR editing in blood cells and assisted with informatic analysis of next generation sequencing data.

MDACC

Name: Marina Konopleva, MD, PhD
Project Role: Site PI (MDACC)
Researcher Identifier (e.g. ORCID ID):
Nearest person month worked: 1 (rounded for this quarter; 0.6 person-months per year)
Contribution to Project: Dr. Konopleva designed and supervised the project

Name: Naveen Pemmaraju, MD
Project Role: Site Co-I (MDACC)
Researcher Identifier (e.g. ORCID ID):
Nearest person month worked: 1 (rounded for this quarter; 0.6 person-months per year)
Contribution to Project: Dr. Pemmaraju worked on development of the clinical protocol.

Name: Lina Han, MD, PhD
Project Role: Site Co-I (MDACC)
Researcher Identifier (e.g. ORCID ID):
Nearest person month worked: 2.4 (rounded for this quarter; 2.4 person-months per year)
Contribution to Project: Dr. Han performed benchwork and analysis of CyTOF data.

Name: Xuelin Huang, PhD
Project Role: Site Co-I (MDACC)
Researcher Identifier (e.g. ORCID ID):
Nearest person month worked: 1 (rounded for this quarter; 0.36 person-months per year)
Contribution to Project: Dr. Huang has supervised biostatistical analysis and assisted with protocol statistical design

Name: Graciela Nogueras Gonzalez
Project Role: Sr. Stat Analyst (MDACC)
Researcher Identifier (e.g. ORCID ID):
Nearest person month worked: 1 (rounded for this quarter; 0.6 person-months per year)
Contribution to Project: Performed biostatistical analysis

Name: Qi Zhang, PhD
Project Role: Postdoctoral fellow
Researcher Identifier (e.g. ORCID ID):
Nearest person month worked: 3 (rounded for this quarter; 3 person-months per year)
Contribution to Project: Dr. Zhang performed in vitro and in vivo experiments

Name: Anna Skwarska, PhD
Project Role: Instructor
Researcher Identifier (e.g. ORCID ID):
Nearest person month worked: 6 (rounded for this quarter; 6 person-months per year)
Contribution to Project: Dr. Skwarska performed in vitro experiments

MSK

Name: Omar Abdel-Wahab, MD
Project Role: Site PI (MSK)
Researcher Identifier (e.g. ORCID ID):
Nearest person month worked: 1 (rounded for this quarter; 0.6 person-months per year)
Contribution to Project: Dr. Abdel-Wahab designed and supervised the project.

Name: Sisi Chen, PhD
Project Role: Postdoctoral fellow
Researcher Identifier (e.g. ORCID ID):
Nearest person month worked: 3 (rounded for this quarter; 3 person-months per year)
Contribution to Project: Dr. Chen performed in vitro and in vivo experiments.

Has there been a change in the active other support of the PD/PI(s) or senior/key personnel since the last reporting period?

Five grants for Dr. Konopleva have completed that were listed on active support in the previous annual report:

Title: Overexpression of CD200 is a Stem Cell- Specific Mechanism of Immune Evasion in AML
Supporting Agency: MDACC Institutional Research Grant
Performance Period: 8/1/2020-7/31/2022
Project Goals: These findings will indicate utility of CD200 as a novel immune checkpoint target for the development of therapeutic strategies against cancer stem cells.
Overlap: None

Title: IMGN632 in BPDCN 1
Supporting Agency: ImmunoGen
Performance Period: 5/5/2019-11/30/2021
Project Goals: IMGN632 in BPDCN 1
Overlap: None

Title: Targeting hypomethylating agent failure in myelodysplastic syndrome
Supporting Agency: Cancer Prevention & Research Institute of Texas (CPRIT)
Name of PD/PI: Colla, Simona
Performance Period: 3/1/2019-2/28/2022
Project Goals: This proposal aims to: 1) functionally validate novel therapeutic approaches to overcome HMA failure in MDS; and 2) identify predictive biomarkers of response and/or resistance to venetoclax in the setting of clinical trials.
Project Number: RP190295
Overlap: None

Title: 2014-0490 LSC assessment Konopleva Lab AML ABT-199 trial
Supporting Agency: AbbVie
Performance Period: 6/1/2020-5/18/2022
Project Goals: Bone marrow aspirate specimens collected from patients on Venetoclax trial in combination with hypomethylating agents (M14-358) will be used for these analyses.
Overlap: None

Title: Targeting Metabolic Rewiring in CLL- Timofeeva

Supporting Agency: CLL Global Research Foundation
Name of PD/PI: Gandhi, Varsha
Performance Period: 3/1/2020-1/31/2022
Project Goals: We want to exploit metabolic nexus of CLL cells. For this we will test agents that target different aspects of metabolism in CLL by targeted small molecule inhibitors of glutaminase, oxidative phosphorylation, etc in CLL cells.

Now active since previous annual report:

None

One grant for Dr. Lane has completed that was listed on active support in the previous annual report:

Title: Novel approaches to AML differentiation therapy
Supporting Agency: Alex's Lemonade Stand
Performance Period: 02/01/18-08/31/22

Now active since previous annual report:

None:

Four grants for Dr. Abdel-Wahab have been completed that were previously listed as active in the prior reporting period:

*Title: Development of therapeutic strategy for the treatment of MDS
*Major Goals: SPECIFIC AIM 1: Elucidate the mechanisms by which mutant p53 alters pre-mRNA splicing in HSCs and MDS cells. Dr. Abdel-Wahab will provide assistance with analysis of splicing in hematopoietic cells with or without mutations in p53. SPECIFIC AIM 2. Determine the impact of inhibition of EZH2 and the spliceosome on MDS cells with TP53 mutations. Dr. Abdel-Wahab will test several therapies targeting RNA splicing in vitro and in vivo in primary human MDS and AML cells with or without mutations in TP5.
*Status of Support: Active
Project Number: 6581-20
Name of PD/PI: Abdel-Wahab, O
Source of Support: Leukemia and Lymphoma Society
Agency Contract: Director of Research Administration, researchprograms@lls.org
Primary Place of Performance: Sloan Kettering Institute For Cancer Research
Project/Proposal Start and End Date (MM/YYYY): 7/1/2019 - 6/30/2022
*Total Award Amount (including Indirect Costs):
Overlap: None

*Title: Understanding the functional implication of cancer-associated mutations in snRNAs (small nuclear RNAs)
*Major Goals: Aim 1: Define the impact of U1 and U11 snRNAs on RNA splicing. Aim 2: Delineate the impact of U1 snRNAs mutations on RNA polyadenylation.
*Status of Support: Completed
Project Number: FP00001800

Name of PD/PI: Abdel-Wahab, O
Source of Support: Functional Genomics Initiative
Agency Contact: Tarsha Barton, bartont@mskcc.org
Primary Place of Performance: Sloan Kettering Institute For Cancer Research
Project/Proposal Start and End Date (MM/YYYY): 8/1/2021 - 7/31/2022
*Total Award Amount (including Indirect Costs):
Overlap: None

*Title: Lineages and pathophysiology of clonal histiocytic disorders
*Major Goals: This project aims to characterize at the molecular, cellular and organismal levels the pathophysiology of clonal histiocytic disorders, exemplified by Langerhans Cell Histiocytosis (LCH) and Erdheim-Chester Disease (ECD).
*Status of Support: Completed
Project Number: 5 R01 HL138090-04
Name of PD/PI: Geissmann, F
Source of Support: National Heart, Lung, and Blood Institute
Agency Contact: Renee Livshin, livshinr@nhlbi.nih.gov
Primary Place of Performance: Sloan Kettering Institute For Cancer Research
Project/Proposal Start and End Date (MM/YYYY): 8/16/2017 - 6/30/2022 (NCE)
*Total Award Amount (including Indirect Costs):
Overlap: None

*Title: Interventional Epigenetics in Myeloid Malignancies
*Major Goals: Our ultimate goal is to define the mechanistic epigenetic basis for the development and progression of myeloid malignancies and to develop novel and effective epigenetic-focused therapies for patients with these disorders.
*Status of Support: Active
Project Number: SPC-001718
Name of PD/PI: Abdel-Wahab, O
Source of Support: Leukemia and Lymphoma Society
Agency Contract: Director of Research Administration, researchprograms@lls.org
Primary Place of Performance: Sloan Kettering Institute For Cancer Research
Project/Proposal Start and End Date (MM/YYYY): 10/1/2017 - 9/30/2022
*Total Award Amount (including Indirect Costs):
Overlap: None

Five new grants for Dr. Abdel-Wahab that are now active:
*Title: Leukemia & Lymphoma Society 2021 CDP Achievement Award
*Major Goals: The CDP Achievement Award was established to recognize awardees who have published the most significant research article(s) and are on clear trajectories to become leaders in the blood cancer field.
*Status of Support: Active
Project Number: LLS_CDP_07_21
Name of PD/PI: Abdel-Wahab, O
Source of Support: Leukemia and Lymphoma Society
Agency Contact: Director of Research Administration, researchprograms@lls.org
Primary Place of Performance: Sloan Kettering Institute For Cancer Research

Project/Proposal Start and End Date (MM/YYYY): 1/1/2022 - 12/31/2022
*Total Award Amount (including Indirect Costs):
Overlap: None

Person Months (Calendar/Academic/Summer) per budget period.

	Year (YYYY)	Person Months (##.##)
1.	2022	0.00 calendar*

*No specified effort required by sponsor.

*Title: Understanding and Overcoming Resistance to Non-covalent BTK Inhibitors
*Major Goals: We hypothesize that the novel BTK resistance mutations identified allow BCR signaling through a scaffold function of BTK and/or by altering proteins physically interacting with BTK. We also hypothesize that these mutations will be sensitive to chemical degraders of BTK.
*Status of Support: Active
Project Number: Mato Greenberg Award 2022
Name of PD/PI: Mato, A
Source of Support: Steven A. Greenberg Startup Grant
Agency Contract: Gilles Salles, MD Chief, Lymphoma Service Department of Medicine, 646-608-2642
Primary Place of Performance: Sloan Kettering Institute For Cancer Research
Project/Proposal Start and End Date (MM/YYYY): 1/1/2022 - 12/31/2022
*Total Award Amount (including Indirect Costs):
Overlap: None

Person Months (Calendar/Academic/Summer) per budget period.

	Year (YYYY)	Person Months (##.##)
1.	2022	0.36 calendar

*Title: Synthetic introns to enable mutation-dependent targeting of cancer cells
*Major Goals: Over the next 2 years, the work proposed here will yield the following milestones: (1) we will develop and optimize delivery of synthetic introns in vivo; (2) we will extend the use of synthetic introns to deliver immunomodulatory molecules for enhanced anti-cancer properties in vivo; (3) and, we will generate synthetic introns responsive to additional recurrently mutated RNA splicing factor genes seen in cancer known as SRSF2 and U2AF1.
*Status of Support: Active
Project Number: ETC Independent Investigator Application
Name of PD/PI: Abdel-Wahab, O
Source of Support: Center for Experimental Therapeutics
Agency Contract: Claudia Little, Program Manager, littlec@mskcc.org
Primary Place of Performance: Sloan Kettering Institute For Cancer Research
Project/Proposal Start and End Date (MM/YYYY): 4/1/2022 - 3/31/2023
*Total Award Amount (including Indirect Costs):
Overlap: None

Person Months (Calendar/Academic/Summer) per budget period.

	Year (YYYY)	Person Months (##.##)
1.	2023	0.12 calendar

*Title: Targeting RNA processing to enhance mucosal melanoma immunotherapy
*Major Goals: Aim 1: Develop a bioinformatic pipeline to identify novel immunogenic targets in MUM following treatment with RNA processing modulators. Aim 2: Identify synthetic promoters specific for SF3B1 mutant MUMs. Aim 3: Modify tumor RNA processing to enhance ICI anti-tumor response.
*Status of Support: Active
Project Number: MRA Team Science Award: #926698
Name of PD/PI: Abdel-Wahab, O
Source of Support: Melanoma Research Alliance Foundation
Agency Contact: Rachel Fischer, 202-336-8929, rfischer@curemelanoma.org
Primary Place of Performance: Sloan Kettering Institute For Cancer Research
Project/Proposal Start and End Date (MM/YYYY): 6/1/2022 - 5/31/2025
*Total Award Amount (including Indirect Costs):
Overlap: None

Person Months (Calendar/Academic/Summer) per budget period.

Year (YYYY)	Person Months (##.##)
1. 2023	0.60 calendar
2. 2024	0.60 calendar
3. 2025	0.60 calendar

*Title: Exploiting Vulnerabilities in RNA Splicing to Treat Hematologic Malignancies
*Major Goals: This consortium will entail performing a phase II trial of E7820 monotherapy for patients with relapsed/refractory myeloid malignancies with mutations in RNA splicing factors and preclinical work
evaluating the impact of altering RNA splicing on immune response.
*Status of Support: Pending
Project Number: 7024-21
Name of PD/PI: Graubert, T
Source of Support: Massachusetts General Brigham / Leukemia and Lymphoma Society
Agency Contact: Jessica Sprague, mghsubs@partners.org
Primary Place of Performance: Sloan Kettering Institute For Cancer Research
Project/Proposal Start and End Date (MM/YYYY): 10/1/2021 - 9/30/2026
*Total Award Amount (including Indirect Costs):
Overlap: None

Person Months (Calendar/Academic/Summer) per budget period.

Year (YYYY)	Person Months (##.##)
1. 2022	0.60 calendar
2. 2023	0.60 calendar
3. 2024	0.60 calendar
4. 2025	0.60 calendar
5. 2026	0.60 calendar

What other organizations were involved as partners?
Nothing to Report

7. SPECIAL REPORTING REQUIREMENTS

COLLABORATIVE AWARDS:

QUAD CHARTS:

8. APPENDICES: